NASA TECHNICAL NOTE

NASA TN D-8062

NASA TN D-8062

EFFECTS OF LONG-CHORD ACOUSTICALLY TREATED STATOR VANES ON FAN NOISE

I - Effect of Long Chord (Taped Stator)

James H. Dittmar, James N. Scott,
Bruce R. Leonard, and Edward G. Stakolich

Lewis Research Center
Cleveland, Ohio 44135

NATIONAL AERONAUTICS AND SPACE ADMINISTRATION • WASHINGTON, D. C. • OCTOBER 1975

1. Report No.	2. Government Accession No.	3. Recipient's Catalog No.
NASA TN D-8062		

4. Title and Subtitle
EFFECTS OF LONG-CHORD ACOUSTICALLY TREATED STATOR VANES ON FAN NOISE
I - EFFECT OF LONG CHORD (TAPED STATOR)

5. Report Date
October 1975

6. Performing Organization Code

7. Author(s)
James H. Dittmar, James N. Scott, Bruce R. Leonard, and Edward G. Stakolich

8. Performing Organization Report No.
E-8331

9. Performing Organization Name and Address
Lewis Research Center
National Aeronautics and Space Administration
Cleveland, Ohio 44135

10. Work Unit No.
505-03

11. Contract or Grant No.

12. Sponsoring Agency Name and Address
National Aeronautics and Space Administration
Washington, D.C. 20546

13. Type of Report and Period Covered
Technical Note

14. Sponsoring Agency Code

15. Supplementary Notes

16. Abstract

A set of long-chord stator vanes was designed to replace the vanes in an existing fan stage. The long vanes consisted of a turning section and axial extension pieces, both of which incorporated acoustic damping material. The acoustic damping material was made inactive for these tests by covering with metal tape, and the stator vanes were tested in three length configurations. Compared to the values for the original stage, broadband noise was reduced in the middle to high frequencies with the long stator vanes, but a broadband noise increase was observed at the low frequencies. No change was observed in the blade passage tone, but some aft end reduction in the overtones was observed.

17. Key Words (Suggested by Author(s))	18. Distribution Statement
Chord length; Fan noise; Noise; Suppressor; Turbofan	Unclassified - unlimited STAR Category 07 (rev.)

19. Security Classif. (of this report)	20. Security Classif. (of this page)	21. No. of Pages	22. Price*
Unclassified	Unclassified	46	$3.75

* For sale by the National Technical Information Service, Springfield, Virginia 22161

EFFECTS OF LONG-CHORD ACOUSTICALLY TREATED STATOR VANES ON FAN NOISE

I - EFFECT OF LONG CHORD (TAPED STATOR)

by James H. Dittmar, James N. Scott, Bruce R. Leonard, and Edward G. Stakolich

Lewis Research Center

SUMMARY

A set of long-chord stator vanes was designed to replace the vanes in an existing full-scale fan stage. These long-chord vanes were designed to investigate the noise reduction possibilities of increased stator chord length. The long vanes consisted of a turning section and axial extension pieces that were added behind the turning section. Acoustic damping material was incorporated in the stator vanes, but the series of tests reported herein are for the cases where the acoustic damping material was made inactive by metal tape. Three stator lengths were tested with both a cylindrical hard wall inlet and a taped (inactive) acoustic inlet.

The broadband noise was affected significantly by the long stator vanes. A noise reduction occurred in the middle to high frequencies, particularly at low fan speeds, probably as a result of the reduced stator response to incoming disturbances. A broadband noise increase was observed at low frequencies, possibly from increased vortex shedding. The broadband noise changes indicate the stator vane area as a significant broadband noise location and therefore a profitable factor for further investigation. No reduction in blade passage tone was observed, presumably because the blade passage tone was controlled by an inlet flow distortion. A decrease in the blade passage overtones was observed toward the rear of the fan, probably a result of reduced vane response to the rotor wakes. The change from a hardwall cylindrical inlet to an inactive acoustic inlet with inactive splitter rings resulted in some tone noise reduction.

INTRODUCTION

One of the noise generation mechanisms in a fan stage is the interaction of the rotor wakes with the downstream stator vanes. Theory indicates that the noise generated by this mechanism can be reduced by increasing the stator vane chord. A set of long-chord stator vanes was designed to replace the stator vanes in an existing 1.83-meter- (6-ft-) diameter, 1.5 pressure ratio fan stage (described in ref. 1) to investigate the noise reduction possibilities of increased stator chord. These stator vanes were tested on the full-scale fan noise test facility at the Lewis Research Center. The long-chord stator design contained 14 stator vanes, whereas the original design contained 112 vanes. Because of the long chord and relatively large thickness, it was possible to incorporate acoustic damping material in these stator vanes. The long acoustically treated stator vanes could thus replace conventional acoustic exhaust splitters. Because of the large thickness involved, such long-chord stator vanes could also replace the struts normally used to carry loads between the engine core and the outer frame.

The data presented here are for the configurations where the acoustic damping material on the stator vanes was made inactive by being covered with metal tape. This report then covers only the acoustic effects of the long stator chord. The effect of the acoustic lining material on the stator vanes will be reported separately.

The taped long-chord stator vanes were tested in three length variations. The shortest length included only the turning section whose chord was approximately 0.61 meter (24 in.) or nine times the chord of the original stator vanes. Two additional lengths were tested by adding extension pieces behind the turning section. The longest version tested had a length of approximately 2.49 meters (98 in.) or 37 times the axial length of the original stator vanes. The longest version of the long-chord stator is shown in figure 1 along with the original stator version it replaced. The acoustic data taken with the various stator lengths are compared with the acoustic data taken with the original stator version to show the effect of chord length.

THEORY

Blade Passage Tone and Harmonics

In the original 1.83-meter- (6-ft-) diameter fan stage, the blade passage tone is believed to come primarily from two sources: the rotor wakes impinging on the stator vanes, and an inlet flow distortion impinging on the rotor blades. The inlet flow distortion appears to be a function of the test installation, as was reported in reference 1.

Rotor-stator interaction. - One purpose of the long-chord stator vanes was to reduce the blade passage tone generated by rotor wake - stator interaction. A number of

researchers have formulated models to predict the noise from this mechanism by calculating the fluctuating lift on the stator vanes as they are struck by the rotor wakes. Examples of these models are given by Kemp and Sears (ref. 2) and Horlock (ref. 3). Portions of some of these models were used in a previous report (ref. 4). An expression for the magnitude of the stator fluctuating lift was indicated in reference 4 (p. 14) as

$$\left|\Delta L_N\right| = \left| \pi\rho \frac{1.6\sqrt{C_D}}{\left(\frac{X}{C_R} + 0.025\right)^{1/2}} U_3 V_1 \sin\left(\bar{\beta}_3 + \beta_3\right) \left[\left|S(\omega)\right| - \alpha \cot\left(\bar{\beta}_3 + \beta_3\right) \left|T(\omega)\right| \right] \right| \tag{1}$$

where

ΔL_N	fluctuating lift, force/area
ρ	fluid density, mass/(length)^3
C_D	rotor profile drag coefficient
C_R	rotor chord
X	distance from trailing edge of rotor to leading edge of stator
U_3	absolute velocity at stator inlet, length/time
V_1	relative velocity at rotor inlet, length/time
β_3	relative flow angle from rotor after translation to stator inlet, deg
$\bar{\beta}_3$	absolute flow angle at stator inlet, deg
α	angle of attack of stators relative to flow, radians
$\left\|S(\omega)\right\|$	magnitude of transverse response function
$\left\|T(\omega)\right\|$	magnitude of longitudinal response function
ω	reduced frequency $\left(\pi C_S/\ell\right)$, radians/time
C_S	stator chord
ℓ	incoming gust wavelength

Since the same rotor was used for both the original 112 vane fan and the long-chord stator fan most of the terms in the expression are the same. With this input, the fluctuating lift expression reduces to

$$\left|\Delta L_N\right| = \left| C_1 \left[\left|S(\omega)\right| - C_2 \left|T(\omega)\right| \right] \right| \tag{2}$$

where C_1 and C_2 are the same for both fans. This expression indicates that any noise reduction should come through the magnitude of $S(\omega)$ and $T(\omega)$.

As indicated, $|S(\omega)|$ and $|T(\omega)|$ are functions of ω, where

$$\omega = \frac{\pi C_S}{\ell}$$

A plot of the reduction of $|S(\omega)|$ and $|T(\omega)|$ with increasing ω is shown in figure 2 from an equation given in reference 3. When the stator chord C_S is increased ω is increased. An increase in ω brings about a reduction in $|S(\omega)|$ and $|T(\omega)|$, thereby indicating a noise reduction. The noise reduction in decibels would be approximately

$$dB_{reduction} = 20 \log_{10}\left(\frac{|\Delta L_N|_{orig}}{|\Delta L_N|_{LCS}}\right)$$

$$= 20 \log_{10}\left(\frac{|\,|S(\omega)|_{orig} - C_2|T(\omega)|_{orig}}{|\,|S(\omega)|_{LCS} - C_2|T(\omega)|_{LCS}}\right) \tag{3}$$

where orig is for original fan and LCS is for long-chord stator.

For estimation purposes, the original fan had an ω of 3.1 at a 100-percent design speed which gives $|S(\omega)|_{orig} = 0.225$ and $T(\omega)_{orig} = 0.645$. The chord of the turning section of the long-chord stator vanes is approximately nine times the chord length of the original stator vanes. This gives $\omega = 27.9$, $|S(\omega)|_{LCS} = 0.075$, and $|T(\omega)|_{LCS} = 0.225$. (These values differ somewhat from those given in ref. 4 since the latter were determined from the tables published in ref. 3 while the values herein were calculated from the equation using a computer.)

With these values of $|S(\omega)|$ and $|T(\omega)|$, the ratios become

$$\frac{|S(\omega)|_{orig}}{|S(\omega)|_{LCS}} = 3.0$$

$$\frac{|T(\omega)|_{orig}}{|T(\omega)|_{LCS}} = 2.9$$

Since the two ratios are so close, for approximation purposes they can be averaged:

$$\frac{|S(\omega)|_{orig}}{|S(\omega)|_{LCS}} \cong \frac{|T(\omega)|_{orig}}{|T(\omega)|_{LCS}} \cong 2.95$$

If both ratios are equal, the expression for the noise reduction reduces to 20 times the log of the ratio. Then the predicted reduction in the rotor wake - stator interaction generated blade passage tone would be

$$20 \log_{10} (2.95) = 9.4 \text{ decibels}$$

It should be noted that the vane-blade ratio was selected to provide the cutoff condition for the blade passage tone in the original design but not for the long-chord stator design. This violation of the cutoff criterion could possibly result in negating the previously predicted reduction of the blade passage tone due to rotor wake - stator interaction for the long-chord stator fan.

Inlet flow distortion. - Reference 1 reports one of the major sources of blade passage frequency noise in this test facility to be the interaction of an inlet flow distortion with the fan rotor blades. An indication of the strength of this inlet flow distortion blade passage noise was given in reference 1 and portions are repeated here in figures 3(a) and (b). These figures show the blade passage tone sound pressure level as a function of angle for two configurations at 90 and 60 percent speeds. The first configuration was with the fan driven through the inlet (the way the tests reported herein were taken) where the distortion was present. The second configuration was with the fan driven from the rear where this installation-caused flow distortion should probably not be present. (The schematics on each figure indicate the front and rear drive configurations.) Since the other noise generation mechanisms were present in both configurations, the comparison shows the relative strength of the inlet flow distortion noise. As can be seen, the sound pressure levels of the tone from the front-drive configuration with the inlet flow distortion were greater than those from the rear-drive version. Since this inlet flow distortion noise was so strong, any possible reduction in the rotor-stator interaction blade passage frequency noise would be masked by the distortion-generated noise and thus probably will not be measured in the far field. However, reductions in the harmonics of the tone and in the broadband level are possible and are now discussed.

Overtones. - The effect of the long-chord stator will most probably be seen in the level of the overtones of the blade passage tone. The data of reference 1 indicate that the overtones of the blade passage tone were not as greatly affected at the rear angles by the incoming distortion as was the blade passage tone. This can be seen in figure 4 where the first overtone is plotted against angle for the same two configurations as

figure 3. (An increase in broadband noise was observed in the rear drive configuration because of flow over supporting structures, etc. The harmonic was not apparent at all of the angular locations because of this extra flow noise and, therefore, no data are present beyond 130°). The effect of the inlet flow distortion on the first overtone was not as strong toward the rear as it was on the blade passage tone and, in fact, at the 120° and 130° angles no increase was noted. (The ability to affect the overtone by influencing rotor-stator interaction parameters was observed previously in a test of rotor-stator spacing on this facility reported in ref. 5.) This observation indicates that the changes in rotor wake - stator generated noise may be observed in the first overtone particularly toward the rear of the fan. The predicted reduction for the first overtone due to rotor wake - stator interaction was accomplished in the same manner as for the tone prediction done previously. This calculation was done with approximately double the reduced frequency parameter ω and resulted in a predicted reduction of approximately 9 decibels. The harmonics for both fans (original and long-chord stators) are not cut off, so no negating effect should be noticed from violating the cutoff criterion.

Broadband Noise

The internally generated broadband noise comes from many sources. These include turbulence interacting with a fan blade, the shed vorticity from a blade, and the scrubbing of the flow over blade surfaces and the fan duct surfaces to name a few. While some of these noise sources should be reduced by the longer stator chord, others should be increased.

The broadband noise generated by turbulence interacting with the stator blades was expected to be reduced by the increased size of the stator chord. Sharland (ref. 6) has indicated the broadband acoustic power that could be generated by an airfoil in turbulent flow. This model used a fixed lift curve slope regardless of the reduced frequency ω. Both Lieppmann (ref. 7) for a general airfoil and Goldstein et al. (ref. 8) for a rotor blade have incorporated a lift response function dependent on the reduced frequency parameter ω. This function is the Sears function $S(\omega)$ mentioned previously. Here again, $\omega = \pi C_S/\ell$, which depends on the blade chord and the incoming gust wavelength. The value of the incoming gust wavelength for incident turbulence is dependent on both the frequency of the turbulence and its convected velocity. Therefore, the amount of broadband reduction achieved by increased stator chord C_S will also depend on the properties of the turbulence. If, for example, turbulence whose frequency is close to the blade passage frequency were convected at the same velocity as the rotor wakes, the predicted reduction would be close to the predicted reduction in blade passage tone due to rotor wake - stator interaction. However, since no measurement of the turbulence striking the stator was made, a prediction of the reduction from the increased stator

chord was not undertaken. It was expected that a broadband noise reduction would be observed as a result of the increased chord and that the amount of reduction should depend on frequency.

The broadband noise generated by scrubbing over the stator surfaces and by the vortex shedding of the stator would probably be increased in the long stator configuration. Other increases in broadband noise could result from separated flow and local shock regions where the flow is contoured around the pylon (not attributable to the concept but possibly observed in the experiment because of test facility constraints).

The net result of all the possible increases and reductions of broadband noise is not readily predictable. However, it would be expected that a reduction in the broadband noise would occur at some frequencies where the turbulence interaction mechanism (or other sources that are reduced by increased ω) was the dominant source, and that an increase would occur at frequencies where other sources were dominant.

APPARATUS AND PROCEDURE

Fan Description

Acoustic data from two full-scale 1.83-meter- (6-ft-) diameter fans differing only in stator design were used for this study. The first fan, shown in figure 5, was a 1.5 pressure ratio, 337.4 meter per second (1100 ft/sec) tip speed fan designated as QF-2 (ref. 1). This fan had 53 rotor blades and 112 stator vanes approximately 6.83 centimeters (2.69 in.) in chord. Other pertinent parameters are listed in table I. Except for the direction of rotation, the QF-2 fan was the same as the QF-1 fan described in reference 9. The acoustic data for the QF-2 fan presented in reference 1 were used as the baseline for deducing the effect of the long stators.

The second fan tested, designated QF-1A, was the long-chord stator design. This fan was tested on the Lewis outdoor fan test facility as a part of the study reported herein. The fan used the QF-1 rotor, which is aerodynamically the same as the QF-2 rotor. The stator vanes of the QF-1A stage bear little resemblance to those of the QF-2 stage, however. There were 14 of the QF-1A stator vanes and they were approximately 61 centimeters (24 in.) in turning section chord. This increased stator chord is the noise reduction feature being investigated. Two additional lengths were tested by adding axial extension pieces behind the turning section. These additional pieces lay in radial planes from the fan centerline.

Long-Chord Stator Design

The long-chord stator vanes were designed to achieve, as closely as possible, the same aerodynamic performance as the original QF-2 stator vanes while achieving a much longer chord. The incorporation of this concept into an existing test facility coupled with the desire for ease of fabrication had considerable impact on the design of these stator vanes.

Test facility requirements. - An illustration of the QF-2 fan nacelle assembly with the original 112 stators is shown in figure 6. The centerbody of the assembly is supported by one large pylon in this test facility. Since it was desired to extend the new long stator vanes to the nozzle entrance, the presence of this thick pylon caused a flow restriction in the fan annulus and dictated the maximum turning-section chord that could be used. Figure 6(a) shows this fan with the cylindrical hardwall inlet, and figure 6(b) shows the fan with an inlet acoustic suppressor including splitter rings which was tested primarily for later comparisons when the stator vane lining material was made active.

Developed view sketches of the fan with the original fan stage and the longest version of the long-chord stators are shown in figures 7(a) and (b), respectively. (All of the rotor blades and stator vanes are not shown on these sketches.) Figure 7(b) shows the arrangement of the long-chord vanes. Those vanes near the pylon are number for reference purposes. As shown in figure 7(b), the trailing edge of stator 5 was faired into the pylon leading edge. With the leading edge of the stator fixed at the same axial location as the leading edge of the QF-2 stators and the trailing edge blending into the pylon, the maximum possible turning section chord was determined.

Because of the flow blockage created by the pylon, it was necessary to terminate stator vanes 4 and 6 on either side of the pylon at the same length as vane 5 leading into the pylon. The incorporation of a slightly longer turning section chord on stator vane 7 (also vanes 1 to 3 and 8 to 14) than on vanes 4, 5, and 6 enabled the area on this side of the pylon to be increased slightly to allow more flow through this channel. On the other side of the pylon, it was necessary to contour stator vane 3 around the pylon to relieve the area restriction. Even with these area redistributions, it was calculated that the channels on either side of the pylon and the channel between stator vanes 2 and 3 would be choked at about the 90 percent speed point of the fan. It should be noted that in flight installations the thickest pylons are much smaller and do not pose a serious problem in applying this concept.

With the chord of the turning section of the airfoil fixed as described and with the desire to retain roughly the same solidity as the original stator, the number of vanes needed was between 13 and 14.

The total blockage area of the vanes upstream of the pylon was also to be retained. The combination of this desired blockage area and expectation that the acoustic lining surfaces would be more efficient at closer spacing led to the choice of 14 stator blades.

Fabrication constraints. - The desire for ease of fabrication of these stator vanes played an important part in the design of the vane turning section. The perforated sheet-over-honeycomb construction used as an acoustic absorber is difficult to machine to a contour and thickness variation required of a conventional stator vane, and it is also difficult to bend in more than one plane. Therefore, it was decided that the general shape of the lined portion of the turning section of a vane would have the same radius of curvature at any radial station from hub to tip (cylindrical section). The leading edge of the stator vanes was then to be a solid piece (no acoustic treatment) which was contoured at each radial station to conform to the incoming flow velocity vector and then blended into the cylindrical lined section.

Construction. - The leading edge section had roughly a NACA-65 series airfoil thickness from the leading edge back to the location where the thickness was equal to the thickness of the lined portion. The thickness was then maintained constant until blended into the lined section. A sketch of a short stator near the pylon (vanes 4 or 6) is found in figure 8(a). Figure 8(b) is a photograph of a completed short stator as it would appear at about 6 o'clock on the fan with the fixture representing the outside wall and with the inside duct wall not shown.

The acoustic lining material used on opposite sides of the stators was of two different thicknesses. These two thicknesses were nominally the same as those used in the exhaust duct of the QF-3 fan (ref. 10). One thickness is placed on each side of the stator so that the different thicknesses face each other across the flow channel formed by two stators. The summation of the two honeycomb thicknesses, two perforated sheets, and the septum thickness determined the overall stator thickness of 3.45 centimeters (1.360 in.). This construction is also shown in figure 8(a). Rivets were used around all edges of the perforated sheet as an easy way to reinforce the epoxy-bonded perforated sheet to honeycomb boundary.

Aerodynamic. - The need to blend one stator vane into the leading edge of the pylon and to have the longer stator vanes proceed straight downstream with extension pieces required that the trailing edge of the turning section of the stator vanes be alined in the axial direction. The original QF-2 stator vanes had turning past axial at some radial locations. The long chord stator vanes are then "under-turned", and in the short version they would probably leave some swirl in the flow.

The previously mentioned aerodynamic and fabrication constraints on the stator design (i.e., contouring around pylon, underturning of flow, cylindrical shape of honeycomb, rivets, etc.) could result in stator losses higher than in an actual engine design not so compromised. In an actual engine the support for the centerbody could come through the stator vanes themselves or a number of small pylons thereby avoiding the high Mach number, high loss region around the large single pylon in the test facility. The rivets on the stator vane surfaces in these high subsonic Mach number flows also contribute to losses that would not be necessary in an actual engine design. As a

consequence of all these compromises, it was recognized that these tests would not yield an accurate evaluation of the aerodynamic performance of the long-chord stator concept.

INSTALLATION AND TEST CONFIGURATIONS

Stator Configurations

Three length increments of the taped long-chord stator were tested. Figure 9(a) shows a photograph of one long stator vane standing on a work table. In this figure, the stator lining material is shown before the tape was applied. The stator vanes were tested in what will be referred to as the short, three-quarter, and long configurations. The short version was just the turning section of each blade and was the length from the leading edge to the first section interface (black section on fig. 9(a)) plus a trailing edge section. The three-quarter version extends to the third section interface from the leading edge (plus the trailing edge). The long version was as shown in figure 9(a). Figure 9(b) shows roughly the length dimensions of the three stator lengths. Figure 9(c) shows a series of sketches of the three stator lengths as they appear in a developed view of the fan rig. It should be noted here that the stator vane leading into the pylon and those on either side of the pylon do not change length.

Figure 10(a) is a photograph of the long stator version installed in the fan rig where the vanes and the inner duct wall have been covered with metal tape. In this photograph the outer cowl has been removed and the fan rotor has not yet been installed. As can be observed, this is the side of the pylon which has the contoured blade. Figure 10(b) is a photograph of the leading edge of the vanes viewed from upstream.

The three-quarter length stator extends to the third black interface from the leading edge in figure 10(a). At this point the vanes were terminated with a contoured trailing edge piece. The short-stator version is seen in figure 11. This photograph was taken during a cleaning procedure between tests. The outline of the long version can be seen on the inner body and the trailing edge of the rotor blades can be seen by looking upstream through the stator.

These three taped stator lengths were tested with two inlets. The first inlet was a cylindrical hard-walled inlet with an inlet bellmouth. The noise from the fan with this inlet was compared with the noise from the fan with the original 112 short stators and the same inlet. The other inlet was acoustically treated with three splitter rings and was tested with the acoustic lining material taped (acoustically inactive). This inlet is the same as described in reference 11 and is tested here as a baseline for later tests when it and the long-chord vanes are made active. The three stator lengths combined with the two inlets mentioned earlier resulted in six test configurations.

Instrumentation

Aerodynamic instrumentation. - Due to restrictions inherent in the facility caused by the large support pylon, the flow in each stator passage was unique. At the time of testing not enough aerodynamic instrumentation was available to measure accurately the flow characteristics in each stator passage. Hence, it was impossible to evaluate the overall aerodynamic performance characteristics of this fan. The instrumentation available was used to determine inlet fan mass flows and to observe localized flow phenomena in suspected problem areas.

The axial locations of the instrumentation are shown in figure 12. In front of the cowl (station 9 in fig. 12), 6 thermocouples placed at uniform circumferential locations (fig. 13(a)) measured the ambient temperature. The inlet static pressure was measured by six wall static pressure taps located at uniform circumferential intervals (fig. 13(b)). For tests run using the hard-walled cylindrical inlet, these pressure taps were located at station 1 in figure 12. For tests run using inlets with splitter rings, the pressure taps were located at station 8 in figure 12.

In the short stator test, aerodynamic rakes containing nine thermocouples and ten total pressure tubes (fig. 14) were placed at various circumferential locations (fig. 15(a)) at the exit plane of the stator passages (station 3, fig. 12). There are wall static pressure taps located on either side of each of these rakes.

The long and three-quarter length stator configurations were tested with the same type of aerodynamic rakes and wall static pressure taps located at various circumferential intervals (fig. 15(b)). However, in these cases the measurements were taken in front of the trailing edge of the support pylon (station 4, fig. 12) and hence well inside the stator passages. In addition to the number of rakes being insufficient to obtain flow characteristics in each stator passage, it was also impossible in this test facility to place the rakes far enough downstream from the stator trailing edge to determine the characteristics of the circumferentially uniform flow or even if the flow was indeed circumferentially uniform.

The tests of the long and three-quarter length stator configurations also incorporated single pitot static tubes in some stator passages (including those nearest the pylon where the flow blockage was greatest) at the plane of maximum support pylon thickness (minimum flow area), station 6 in figure 12.

Acoustic instrumentation. - Far field acoustic data were obtained by 1.27-centimeter- (0.5-in.-) condenser microphones located on an arc at 10° increments from 10° to 160°. A photograph of the test site and a plan view of the microphone locations are shown in figure 16. The microphones were level with the fan centerline, 5.79 meters (19 ft) above the ground on a 30.48-meter (100-ft) radius. A complete description of the acoustic instrumentation and the data acquisition techniques is given in reference 9.

Three samples of acoustic data were taken at each test condition and averaged to minimize the effect of short-term fluctuations in the generated noise. The data taken at 60, 70, 80, and 90 percent of design speed were recorded on magnetic tape; both a one-third octave band analysis and some constant band width narrow band analyses were performed.

RESULTS AND DISCUSSION

As mentioned previously, three taped lengths of the long-chord stator vanes were tested. The first section, referred to as the short stator configuration, consisted only of the turning section of the stator. The next two sections, referred to as the three-quarter and long stator configurations, consisted of the turning section of the stator vane plus extension pieces on most of the stator vanes (see fig. 9(c)). Each of these stator vane lengths was tested with two different inlets. These inlets, which included an inlet bellmouth, were a cylindrical hard-walled inlet and a taped (inactive) acoustic inlet including three taped (inactive) acoustic splitter rings.

The results of these tests are presented in two parts, the aerodynamic results and the acoustic results. The acoustic results are then presented in two main parts corresponding to each inlet tested.

Aerodynamic Results and Discussion

Again it must be mentioned that available instrumentation was insufficient to determine the overall aerodynamic performance characteristics of the long-chord stator fan stage (QF-1A). Hence, only localized flow effects are discussed.

The wall static pressure measurements taken in the fan inlet were used to calculate corrected inlet mass flow. The corrected inlet mass flow is plotted against percent of design speed in figure 17. In this figure, the dashed lines show how inlet mass flow varies with fan speed for QF-2 with the design nozzle and with the design exit nozzle area increased by 10 percent. The behavior of the QF-1A inlet mass flow, an average of both short and long stator version data (fig. 17), with increasing fan speed indicates that there is a relative falloff with speed for QF-1A with respect to QF-2. This falloff is possibly a result of a falloff with speed of exit total pressure, effective nozzle area, rotor operating point, or a combination of these effects.

Since the inlet mass flow for QF-1A was closer to that of QF-2 with the design nozzle at higher fan speeds, this configuration of QF-2 is used as the basis of comparison for the noise data. Each data point in figure 17 represents an average of all data taken for the specified fan-nozzle configuration at the given speed. The QF-1A inlet mass

flow was relatively independent of inlet configuration and long-chord stator length variations.

In the short-stator configuration, the gage pressure measured with the total pressure tubes of rake "C" at the exit plane of the stator passage indicates the presence of a region of separated flow in the passage between stator 7 and the pylon. This region was near the trailing edge of stator 6 (see fig. 7). A plot of radial pressure distribution is shown in figure 18. This figure shows how this region of separation grew with increasing fan speed and that it occurred near the centerbody of the fan duct. Radial pressure distributions from other rakes (station 3, fig. 19) show that this separation was localized near the pylon in the short stator configuration. Insufficient instrumentation prevented determining how this disturbance propagates downstream.

In the long and three-quarter length stator configurations the pitot static tubes at the plane of minimum flow area provided the data for calculating flow Mach numbers in some of the more critical stator passages. The Mach numbers at 90-percent speed ranged from values as low as 0.6 in passages away from the support pylon to values as high as 0.92 in passages near the pylon (those passages containing area contractions due to the presence of the pylon and special contouring of the vanes).

The total pressure rake measurements at station 4 just upstream of the pylon trailing edge are shown in figure 20. These measurements indicate significant differences between the total pressures measured for the different rake locations. Those total pressure differences along with the Mach number variations noted previously tend to indicate that some of the stator passages were acting as converging-diverging nozzles and thus may have been choked at the higher fan speeds. It is believed that this behavior resulted in a redistribution of flow in the nonchoked stator passages. This result further indicates that the flow through each stator passage was unique.

It is evident from the data collected that to evaluate the overall aerodynamic characteristics of this fan much more extensive instrumentation would be required. Specifically, it would be necessary to measure total pressure profiles in both radial and circumferential directions in each stator passage in order to obtain the performance losses. However, the falloff of the inlet mass flow of QF-1A with respect to QF-2 (fig. 17) may indicate that additional total pressure losses do exist in these long stator configurations. The mass flow reduction in the short stator version is quite possibly a result of losses associated with the separated flow region near the pylon. In the long stator version the mass flow falloff may result from a reduction in the nozzle effective area because of the proximity of the long stator trailing edge to the nozzle entrance and/or from added losses from flow over the large stator surface area.

Acoustic Results

Cylindrical hardwall inlet. - The cylindrical hardwall inlet cases were run to provide comparisons of the generated noise from the various lengths of the taped long-chord stator with the generated noise from the original stator vanes. Figures 21 to 23, show the general data taken with the three lengths of the long-chord stator. These plots give one-third octave band acoustic power spectra for 60, 70, 80, and 90 percent of fan design speed. Figure 21 is for the long stator vane configuration, figure 22 the three-quarter length configuration, and figure 23 the short configuration.

The three figures show very similar results in that the noise increased as the speed was increased. The plots for the long and three-quarter configurations are almost identical at all speeds (some differences are noted as the result of different test speeds), but the short configuration provided significantly more broadband noise than either the three-quarter or long configurations. To better illustrate this point, data from the three configurations are plotted together in figure 24. Figure 24(a) is for 90 percent speed and figure 24(b) is for 60 percent. The spectra for the three-quarter and long configurations are almost identical and the small differences are probably scatter in the data. The levels from the short configuration of the long-chord stator were higher at frequencies below the blade passage frequency. This broadband increase was more noticeable at the lower speed points than at the high ones, probably because the increase was overshadowed by other sources at the high speed points. This broadband noise increase is believed to be due to the separated flow region observed in the aerodynamic testing. The separated flow region associated with the flow around the suction surface of the pylon (between stator 7 and the pylon on fig. 7) is not necessarily a fault of the concept but only of an imperfect accommodation to restrictions imposed in this particular test facility. This region did not appear with the longer configurations of the stator because of the extension of stator 7 in these configurations (see fig. 7).

The short configuration of the long-chord stator will not be compared acoustically with the original stator vane data since the additional broadband noise, above the three-quarter or long versions, observed at the low frequencies is not attributable to the long-chord stator concept. Since the three-quarter and long configurations of the long-chord stator gave approximately the same noise spectra, only the long configuration data are compared with the original conventional stator data.

Figure 25 shows a series of comparisons between the acoustic power for the original short-chord stator vanes (QF-2) and the acoustic power for the long configuration of the long-chord stator vanes. Figure 25(a) is for 60 percent, 25(b) for 70 percent, 25(c) for 80 percent, and 25(d) for 90 percent of design speed. A number of things are noteworthy about this series of comparisons. As indicated previously (THEORY section), the inlet flow distortion - rotor interaction mechanism appears to be the dominant source of blade passage frequency noise. In this testing the blade passage tone was not

changed with the long-chord stator vanes (fig. 25(a) to (d)). (The slight change at 90 percent is just a slight shift in one-third octave band as a result of day to day fan speed changes to obtain constant corrected speeds; when the power is added in two bands the levels are the same.) As anticipated, any blade passage frequency noise reduction that occurred from the change to the long-chord stator vanes is not visible probably because the blade passage tone generated by the inlet flow distortion is masking the effect.

The first overtone of the blade passage frequency does show some noise reduction as a result of the change to the long-chord stator. On acoustic power, this effect was more noticeable at the lower speeds than at the higher speeds. Part of the reason for this is that the inlet flow distortion contribution to the overtone was not as strong at the low speeds and changes in the rotor wake - stator noise generation were more easily seen. In addition, the one-third octave band containing the first overtone also contains broadband noise which may contribute to the signal level. To better investigate the effect on the overtone, a number of narrow band spectra were taken. The level of the harmonic was determined from three samples of narrow band spectra at each azimuth angle. A plot of this harmonic as function of angle along with the QF-2 original stator data is shown in figure 26 for 90 percent speed. As can be seen, the first overtone was about the same in the front from 10^{o} to 70^{o}. This is a further indication that the inlet flow distortion controlled the first overtone in the front. However, noise reductions are observed in the rear beyond 80^{o} where the rotor wake - stator interaction could be dominant. In fact, beyond 100^{o}, the first overtone has been reduced below the level of the broadband noise which in this region is represented with different symbols. To further show this result, three narrowband spectra are presented in figure 27 at 50^{o}, 80^{o}, and 120^{o} to show the differences between the front and rear radiated noise. (The sound pressure levels in these spectra may not correspond to those of fig. 26 since the levels on fig. 26 are the average of three narrowband spectra.) As can be seen, there was little change in the level of the overtone in the front (50^{o}, fig. 27(a)), but it was reduced toward the rear (80^{o}, fig. 27(b)) and had disappeared into the broadband at the 120^{o} microphone (fig. 27(c)). The second overtone was reduced with the long-chord stator vanes as can be observed in this series of narrowbands. The reductions in the overtones are not as great as the 9 decibels predicted by the theory. This discrepancy may be due to the presence of inlet distortion noise, or, for the rear angles, it may be due to the presence of a broadband noise floor. Nevertheless, a reduction in the first and second blade passage frequency overtones has been shown as a result of the long-chord stator vanes and even more reduction might be expected if other noise sources such as the inlet distortion were not present.

When returning to figure 25 the reader observes a significant effect of the long-chord stators on the broadband noise. Starting with 60 percent speed (fig. 25(a)), the broadband noise was greatly reduced above 630 hertz with the long-chord stators while only a slight increase was observed below 500 hertz. This noise reduction at 60 percent

speed would be most effective during an airplane's landing approach. As the fan speed was increased, the noise source generating the increased low frequency noise became stronger and the emission occurred over a broader range of frequency until at 90 percent (fig. 25(d)) the increase was observed in the 200 to 1600 hertz range. The reduction in the high frequency broadband noise was still observed above the blade passage frequency but it was not as strong a reduction at this 90 percent speed point.

To obtain an indication of where the noise sources are acting, the generated sound power was split into front and rear hemisphere power levels. Data at 80 percent speed show more clearly than data at other speed points the apparent split of where the noises are emanating. Figure 28(a) shows the front quadrant, and figure 28(b) shows the rear quadrant. As can be seen by this figure, the reduction in the broadband noise was mostly in the front, and the increase at the lower frequencies was mostly in the rear.

For additional clarity, two broadband sound pressure level plots of specific one-third octave bands are shown in figure 29. Figure 29(a) shows the angular sound pressure level variation in the one-third octave band centered at 3150 hertz that was reduced with the long-chord stator, and figure 29(b) shows one of the bands which showed an increase, 630 hertz. These data are both for 80 percent speed to correspond with figure 28. In viewing figure 29(a), the decrease in broadband noise with the long-chord stator vanes is seen to occur toward the inlet of the fan (from 10° to 120°). This forward radiated broadband noise is probably radiated from the front of the long-chord stator vanes. This general location is where the incoming turbulence or rotor wake irregularities would generate fluctuating lift on the stator vanes. This fact points to the longer chord reducing the response of the stator to the incoming disturbances, thereby reducing the broadband noise in this frequency range. This same effect of more noise reduction in the front can be seen in the narrow band traces of figure 27 where the 50° and 80° mikes show marked broadband noise reductions but the 120° microphone shows little. In fact, the narrow bands may give a better feel for the amount of sound power reduction since the one-third octave plots emphasize the low frequency part of the spectrum while the narrow band spectra emphasize all frequencies equally. From a subjective point due to the sensitivity of the ear the decrease in the high frequency noise may be more important than the increase at the lower frequencies.

Figure 29(b) shows the variation of one of the one-third octave bands where the noise was increased with the long-chord stators. In the figure it is seen that the increase in low frequency broadband noise occurred mostly toward the rear of the fan, from 70° back. This increase probably occurred on the rear portion of the long-chord stator or possibly in the exhaust jet and is an indication that the cause may be increased vortex shedding from the long-chord stator at these low frequencies or, possibly, an increase in jet noise because of increased turbulence in the jet.

To summarize, the decrease of broadband noise observed in the high frequencies was probably a result of the longer stator chord reducing the response of the stator

vanes to the incoming turbulence or rotor wake nonregularities. The increase in noise at the low frequencies was possibly the result of vortex shedding from the long-chord stator vanes or an increase in jet noise from increased turbulence. The ability to impact the broadband noise output of the fan (particularly the reduction) presumably by only changing the stator indicates, at least in this fan stage, that the stator controlled the broadband noise. This conclusion, if applicable to other fans, could have a significant effect on future efforts to reduce broadband noise generation.

Taped inlet with taped rings. - In general, the taped inlet with taped stator vane tests were run for later comparisons with the configuration where the stator treatment was made active. A number of interesting effects were noted, however. Figures 30 to 32 show power spectra for the three long-chord stator lengths with the taped inlet with rings: figure 30 is for the long configuration, figure 31 the three-quarter configuration, and figure 32 the short configuration. Each figure contains four curves corresponding to the 60, 70, 80 and 90 percent speed points.

As can be seen by comparing these figures with figures 21 to 23, the total power radiated with either of the inlets was almost the same. The one exception seemed to occur around the blade passage frequency of the fan. For direct comparison, the 90 percent speed long stator configurations are plotted in figure 33. As can be seen, the blade passage noise was reduced with the taped inlet. Since the blade passage tone was presumed to be controlled by the inlet flow distortion, this may indicate that the inlet rings serve to break up the incoming distortion and reduce the blade passage tone energy.

Despite the fact that the total radiated power, at frequencies other than blade passage, was almost the same for both the cylindrical hardwalled inlet with no rings and the taped inlet with rings, there are significant differences in the fan noise. To illustrate these differences, two one-third octave bands are plotted against angle in figure 34. These are again for the 90 percent speed long stator configurations. The 2500-hertz center frequency band plot (fig. 34(a)) indicates the blade passage tone level, but since the tone energy is partly in this band and partly in the adjacent 3150-hertz center frequency band it is not the total blade passage tone. As seen here, the reduction in this one-third octave band was in the front of the fan while the rear ($>100^{o}$) was almost unaffected. This further indicates that the inlet rings reduced the blade passage tone, possibly through the partial elimination of the inlet flow distortion.

The one-third octave band centered at 1000 hertz (fig. 34(b)) gives an indication of the fan broadband noise. The broadband noise, as indicated by this figure, was also reduced slightly in the front of the fan. This reduction did not appear in the total power plots seen previously because the rear radiated noise of the fan controlled the broadband noise at this frequency. Both of the plots in figure 34 indicate that the taped inlet with rings reduced the forward radiated noise. This is possibly the result of flow smoothing provided by the inlet rings. The effect of taped inlet rings was previously observed in

reference 10 but only a shift in directivity was observed in that report and not the reduction in forward-radiated noise as observed here. For this reason, the reduction of noise with taped inlet rings is not a general result.

CONCLUDING REMARKS

A set of long-chord stator vanes was designed to replace the conventional vanes in an existing full-scale fan stage. These vanes were tested in three lengths, first with just the turning section of the blades and then with additional axial extension pieces. Although the vanes had acoustic lining material on their surfaces, the surfaces were inactivated with metal tape for the tests described herein. The three vane lengths were tested with two different inlets, namely, a cylindrical hardwalled inlet and a taped acoustic inlet with taped rings. The following results were obtained:

1. When comparing the blade passage tone generated with the taped long-chord stator vanes with that of the original short-chord stator vanes no change was observed. Theory indicates that the rotor wake - stator interaction generated blade passage tone should have been reduced by the increased chord of the long-chord stator vanes. The fact that no blade passage tone reduction was observed was probably because an inlet flow distortion - rotor interaction generated noise was the dominant tone source and masked any reduction in rotor wake - stator interaction generated noise. This inlet flow distortion is an installation effect of this test facility, and a reduction in blade passage tone as a result of a longer stator chord might occur in a test facility where this inlet flow distortion was not present.

2. Reductions in the overtones of the blade passage tone were observed with the long-chord stator vanes. These reductions were mostly toward the rear of the fan where the inlet flow distortion - rotor interaction noise did not dominate the overtones. In fact, at angles greater than 100^{o}, the first overtone was reduced below the level of the broadband noise. This result provides some evidence for reducing tone noise by longer stator chords, even though the reductions observed were not as great as predicted by the rotor wake - stator interaction theory.

3. The broadband noise output of the fan was greatly affected by the long-chord stators. At the medium to high frequencies the broadband noise was significantly reduced in comparison with the original stators, probably as a result of the long stator chord reducing the stator response to incoming turbulence and unsteady blade wakes. A noise increase was observed at low frequencies probably as a result of increased vortex shedding from the long-chord stators. This noise increase was hardly noticeable at low speeds but continued to grow in magnitude and frequency until it was significant at 90 percent speed. A portion of this noise increase may be the result of aerodynamic compromises made to incorporate the fan in the existing test facility. The shortest

version of the long-chord stators also exhibited some additional broadband noise probably from an identified flow separation in the channel near the pylon. This flow separation was at least in part the result of compromises made to adapt the long-chord stator concept for installation in the test facility.

4. The changes observed in the broadband noise, particularly the reductions, indicate that the stator controlled the broadband noise, at least in this fan. This further points to the stator as a profitable area for investigating broadband noise reduction.

5. Tests run with a taped inlet with taped rings showed a noise decrease relative to tests with a hardwall cylindrical inlet with no rings. This reduction was mostly in the front hemisphere and was more pronounced at the blade passage frequency. The noise reduction was probably the result of the rings reducing the inlet flow distortion, thereby reducing the generated noise.

Lewis Research Center,
National Aeronautics and Space Administration,
Cleveland, Ohio, June 17, 1975,
505-03.

REFERENCES

1. Povinelli, Fredrick P.; Dittmar, James H.; and Woodward, Richard P.: Effects of Installation Caused Flow Distortion on Noise from a Fan Designed for Turbofan Engines. NASA TN D-7076, 1972.

2. Kemp, Nelson H.; and Sears, W. R.: The Unsteady Forces Due to Viscous Wakes in Turbomachines. J. Aeron. Sci., vol. 22, no. 7, July 1955, pp. 478-483.

3. Horlock, J. H.: Fluctuating Lift Forces on Aerofoils Moving Through Transverse and Chordwise Gusts. J. Basic Eng., vol. 90, no. 4, Dec. 1968, pp. 494-500.

4. Dittmar, James H.: Methods for Reducing Blade Passing Frequency Noise Generated by Rotor-Wake-Stator Interaction. NASA TM X-2669, 1972.

5. Balombin, Joseph R.; and Stakolich, Edward G.: Effect of Rotor-to-Stator Spacing on Acoustic Performance of a Full-Scale Fan (QF-5) for Turbofan Engines. NASA TM X-3103, 1974.

6. Sharland, I. J.: Sources of Noise in Axial Flow Fans. J. Sound Vib., vol. 1, no. 3, July 1964, pp. 302-322.

7. Lieppmann, H. W.: On the Application of Statistical Concepts to the Buffeting Problem. J. Aeron. Sci., vol. 19, no. 12, Dec. 1952, pp. 793-800, 822.

8. Goldstein, Arthur W.; Glaser, Fredrick W.; and Coats, James W.: Effect of Casing Boundary-Layer Removal on Noise of a Turbofan Rotor. NASA TN D-6763, 1972.

9. Leonard, Bruce R.; Schmiedlin, Ralph F.; Stakolich, Edward G.; and Neumann, Harvey E.: Acoustic and Aerodynamic Performance of a Six-Foot-Diameter Fan for Turbofan Engines. I - Design of Facility and QF-1 Fan. NASA TN D-5877, 1970.

10. Dittmar, James H.; and Groeneweg, John F.: Effect of Treated Length on Performance of Full-Scale Turbofan Inlet Noise Suppressors. NASA TN D-7826, 1974.

11. Rice, Edward J.; Feiler, Charles E.; and Acker, Loren W.: Acoustic and Aerodynamic Performance of a Six-Foot-Diameter Fan for Turbofan Engines. III - Performance with Noise Suppressors. NASA TN D-6178, 1971.

TABLE I. - DESIGN VALVES FOR QF-2 FAN

Rotor tip diameter, m (in.)	1.824 (71.81)
Stator tip diameter, m (in.)	1.726 (67.94)
Rotor tip speed (cruise design value, corrected), m/sec (ft/sec)	337.4 (1107)
Design stagnation pressure ratio	1.5
Design weight flow (corrected), kg/sec (lbm/sec)	396 (873)
Rotor hub-tip radius ratio (inflow face)	0.50
Stator hub-tip radius ratio	0.59
Rotor-stator spacing (rotor trailing edge to stator leading edge at the hub), cm (in.)	50.8 (20)
Number of rotor blades	53
Number of stator blades	112
Rotor chord length, cm (in.)	13.97 (5.5)
Stator chord length, cm (in.)	6.83 (2.69)

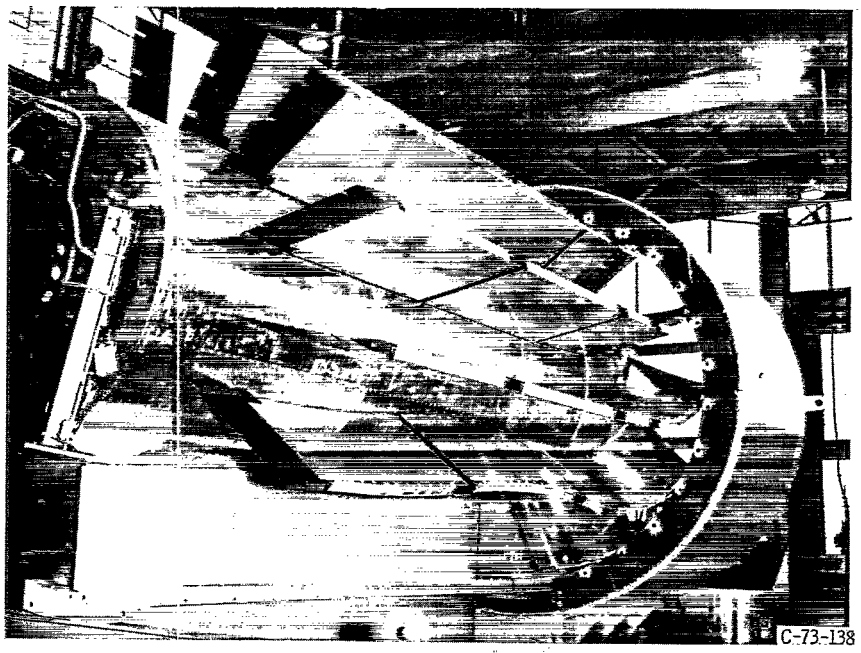

(a) Long-chord stator (longest version).

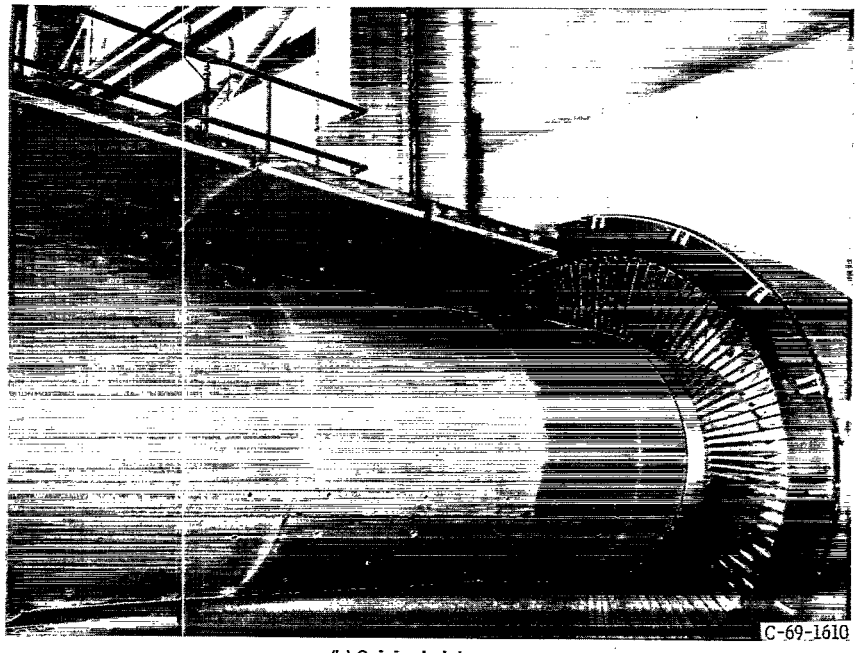

(b) Original stator vanes.

Figure 1. - Fan stator vanes (viewed from downstream).

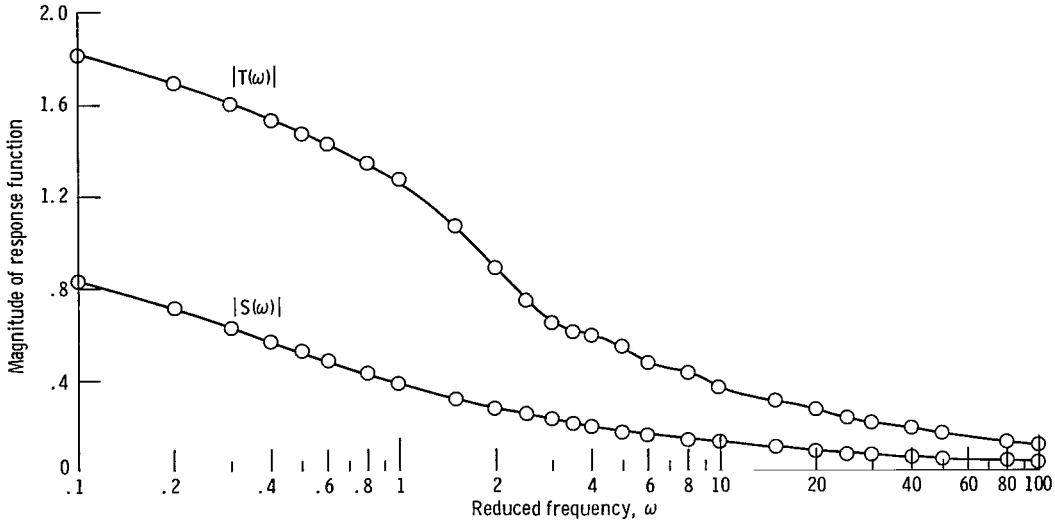

Figure 2. - Changes in magnitudes of transverse and longitudinal response functions with changes in reduced frequency (from eqs. given in ref. 3).

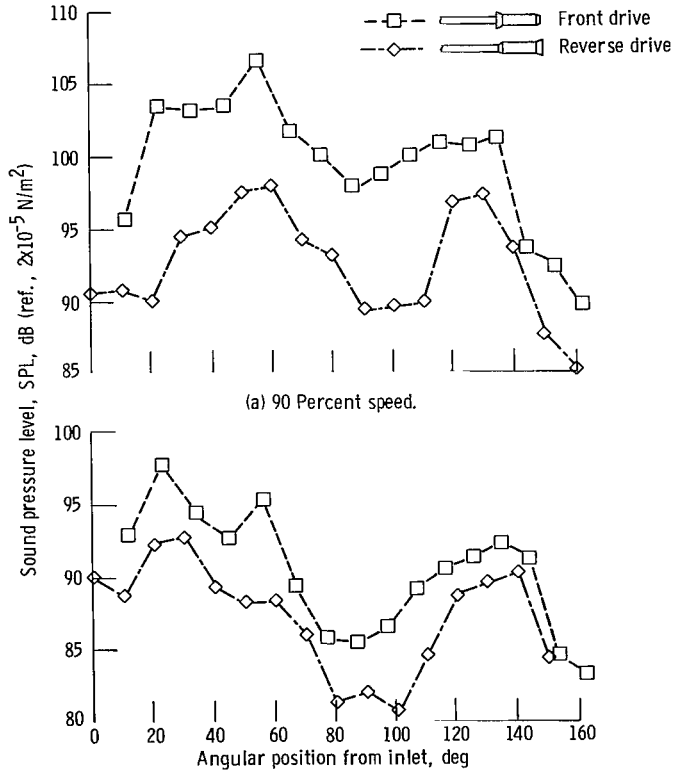

Figure 3. - Angular distribution of blade-passage tone from narrow-band spectra on 30.5-meter (100-ft) radius. (Standard-day conditions from ref. 1.)

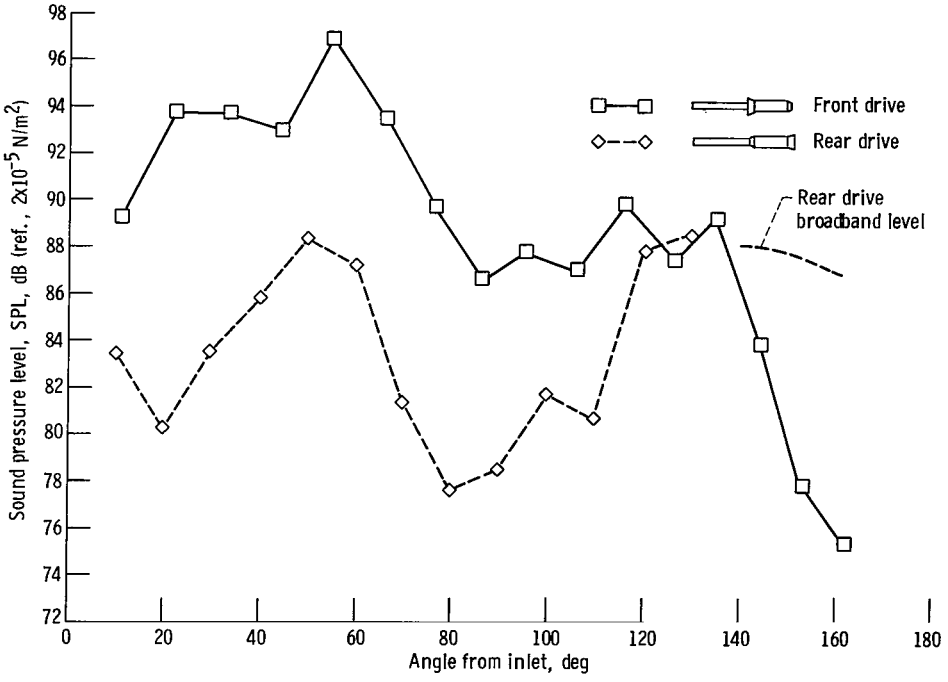

Figure 4. - Angular distribution of first overtone from narrowband spectra on 30.5-meter (100-ft) radius for 90 percent speed.

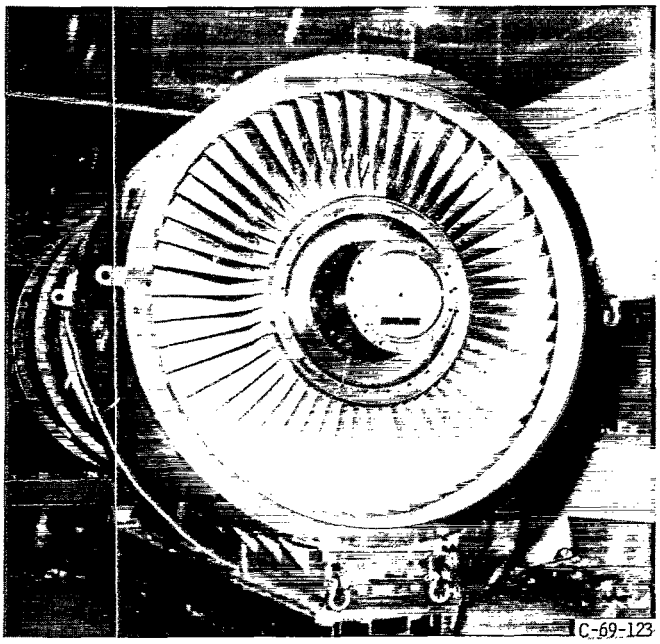

(a) Rotor.

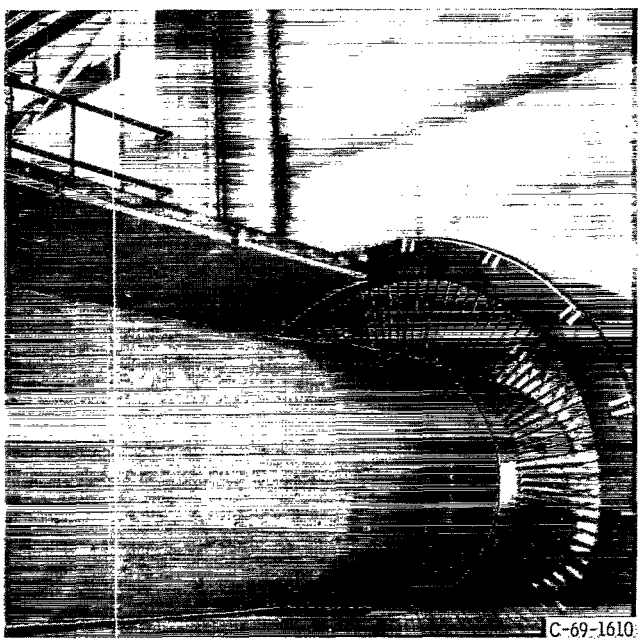

(b) Stator.

Figure 5. - QF-2 fan.

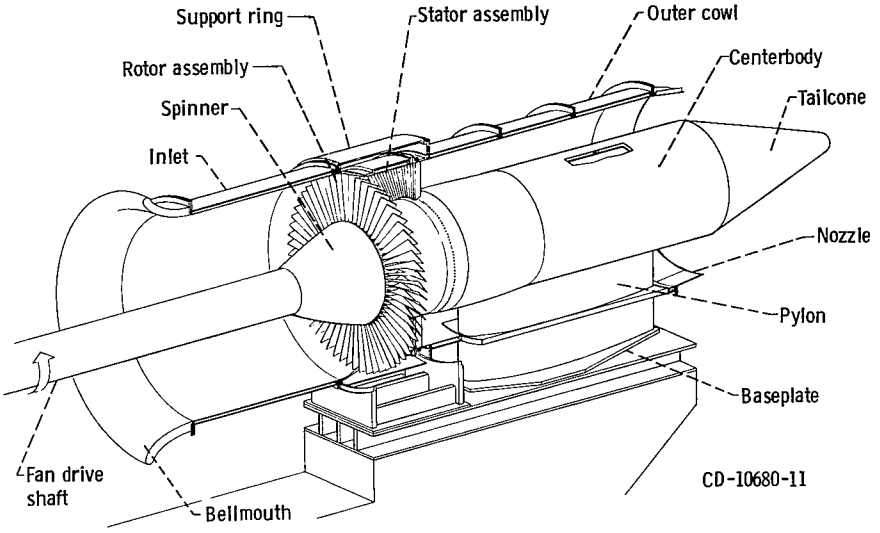

(a) Cylindrical hardwall inlet.

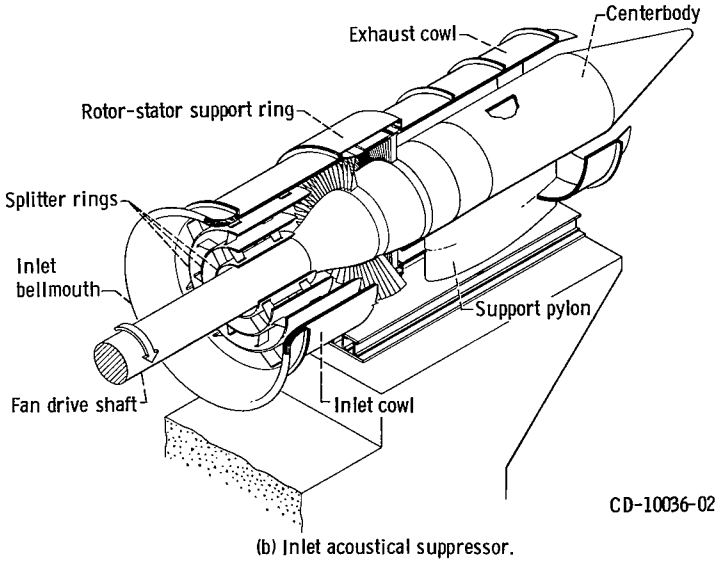

(b) Inlet acoustical suppressor.

Figure 6. - QF-2 fan nacelle assembly.

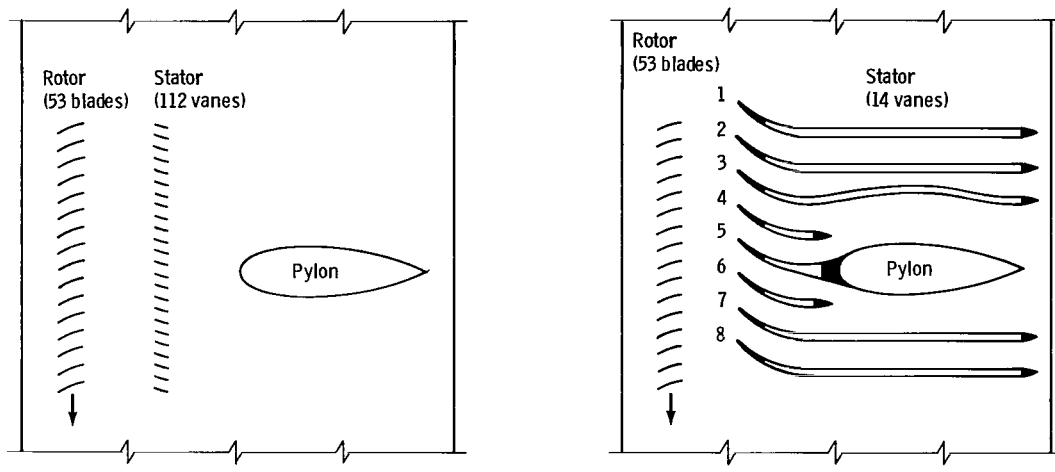

(a) Original fan stage.

(b) Fan stage with long-chord acoustically treated stator.

Figure 7. - Developed views of fan stages.

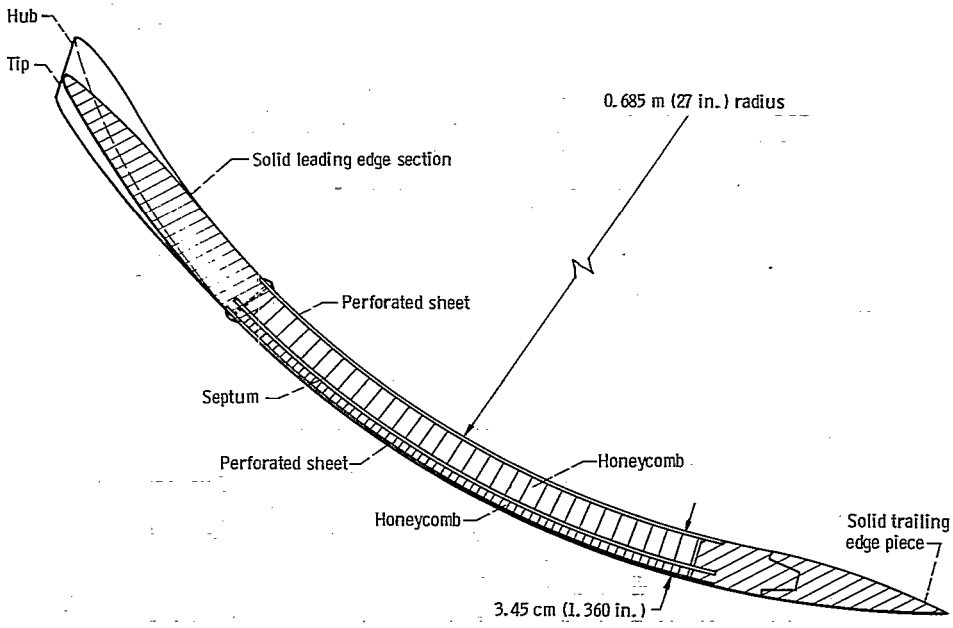

(a) Cross-sectional sketch.

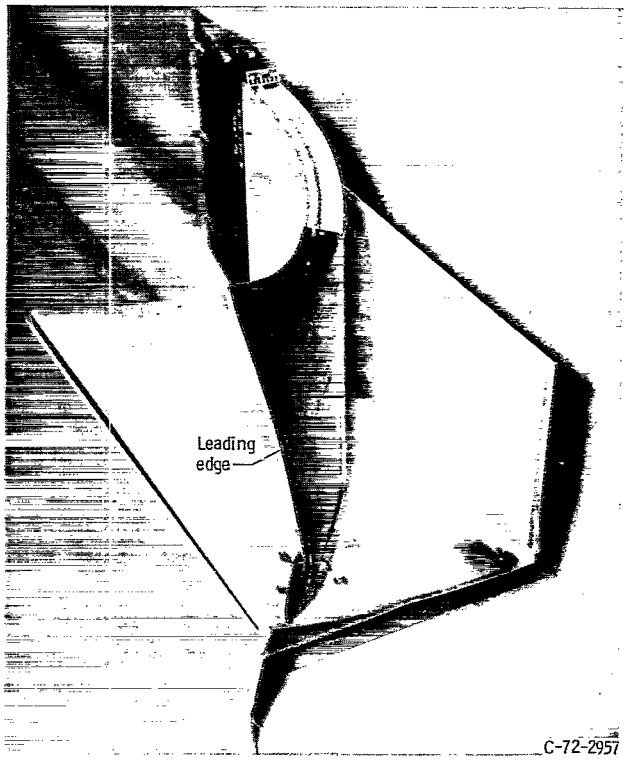

(b) Short stator on work table.

Figure 8. - Short stator configuration.

(a) Long stator on work table.

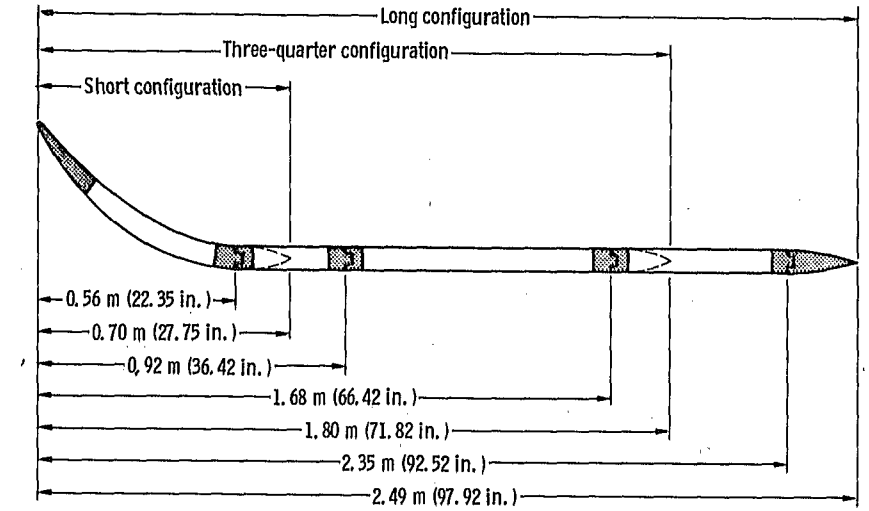

(b) Stator length variations.

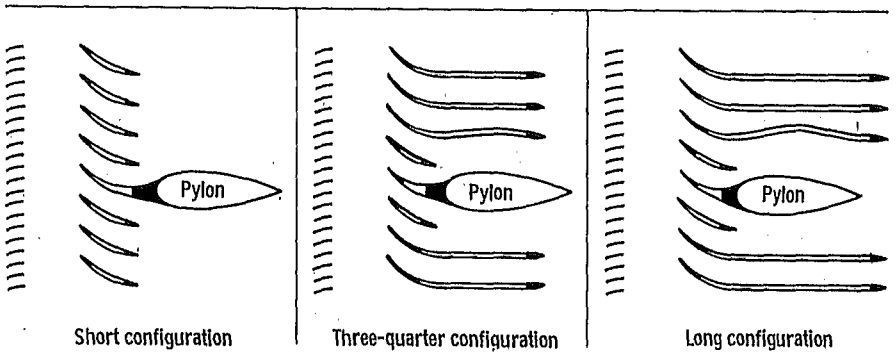

(c) Developed views of length variations.

Figure 9. - Long stator configuration.

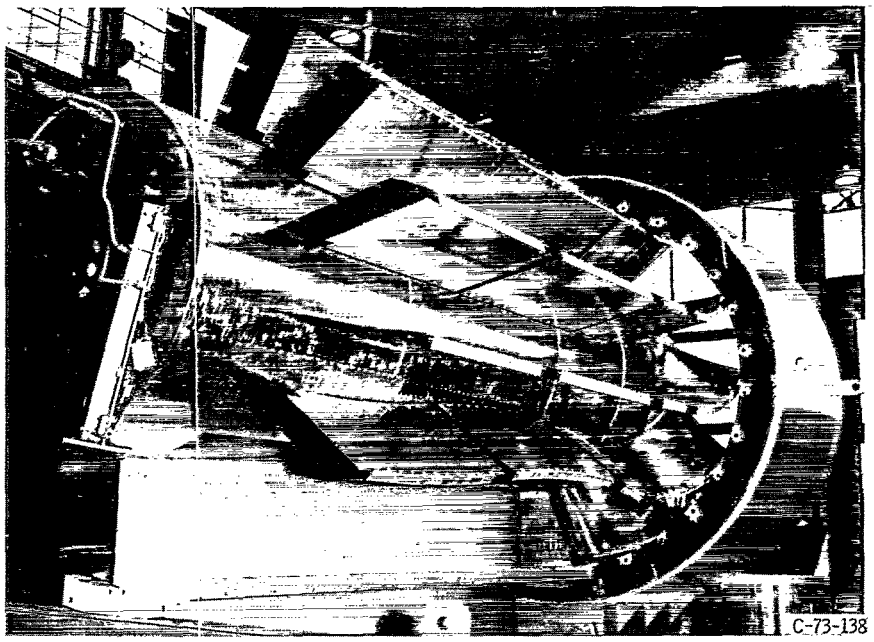

(a) View looking forward.

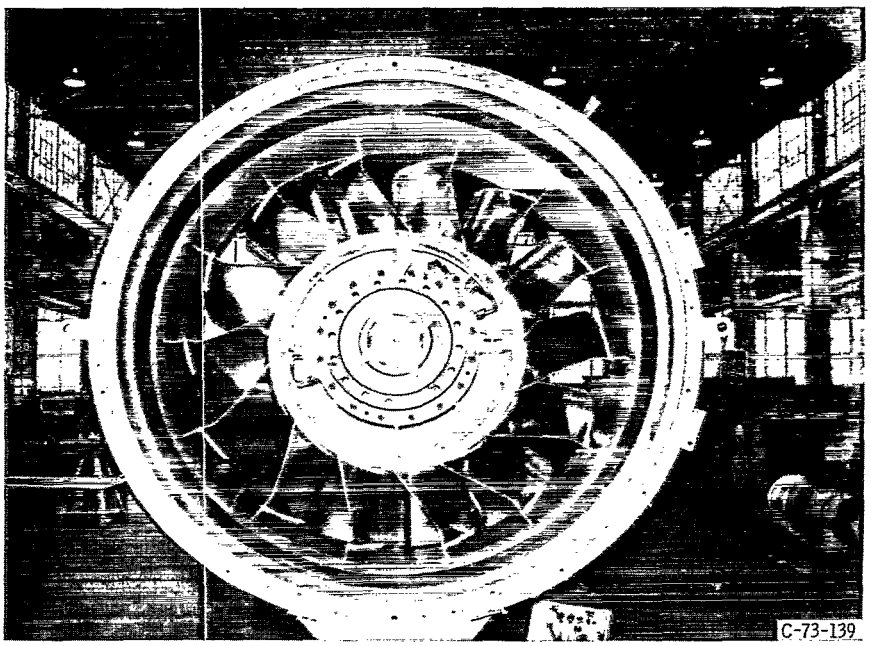

(b) Looking at stator leading edge.

Figure 10. - Taped long stator during installation in test nacelle.

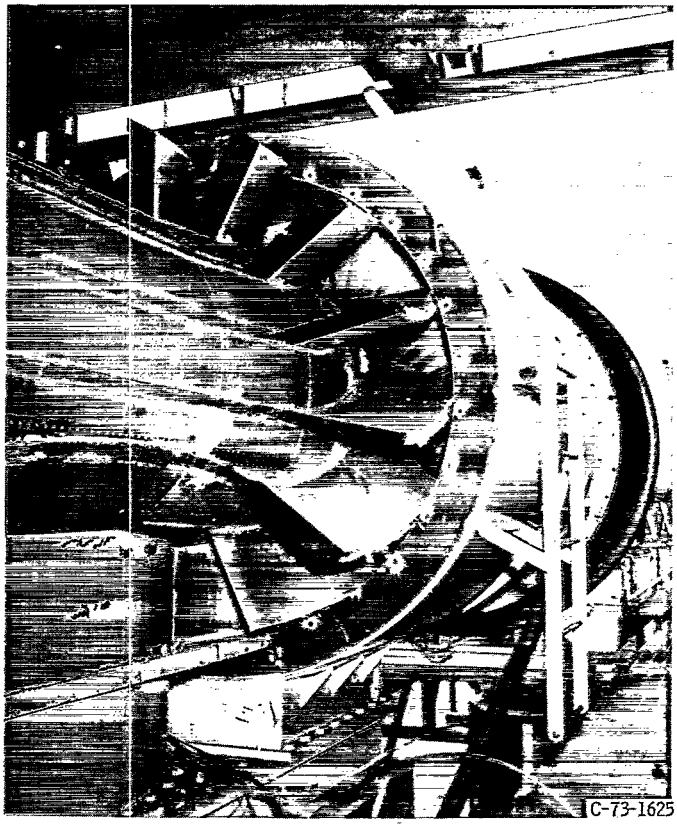

Figure 11. - Short stator configuration in test facility.

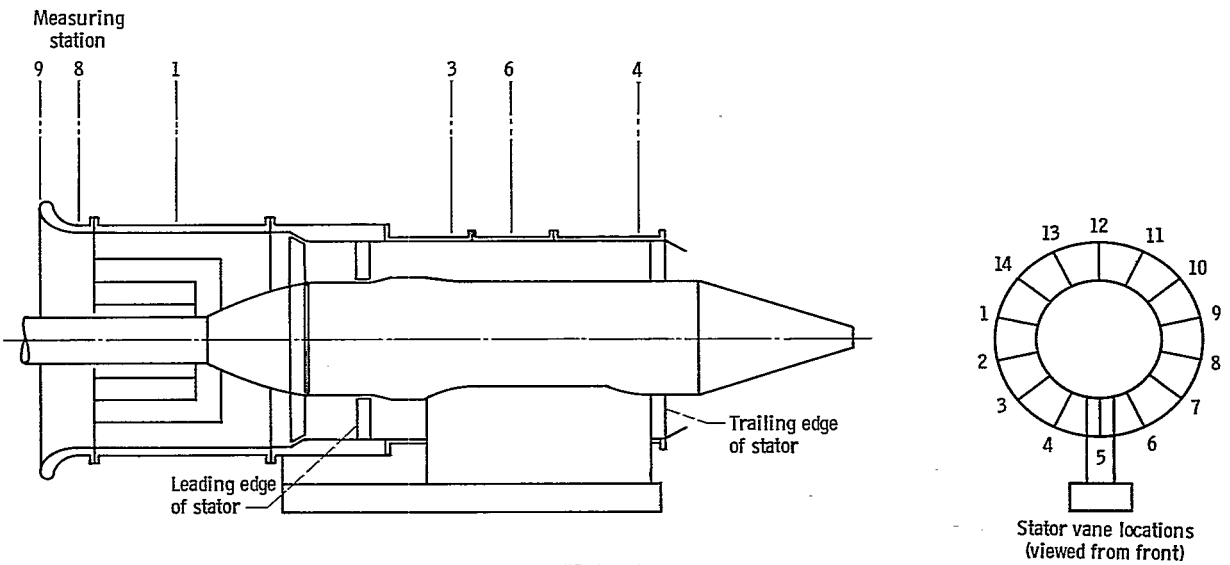

Figure 12. - Long-chord stator instrumentation locations.

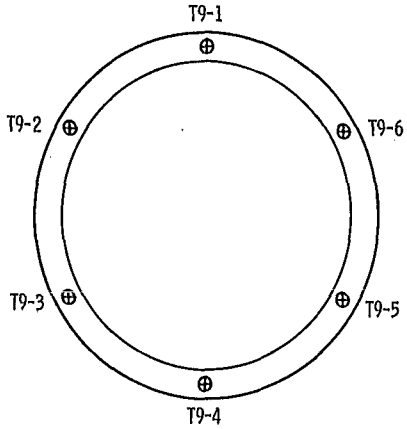

(a) Thermocouples for inlet air temperature (station 9).

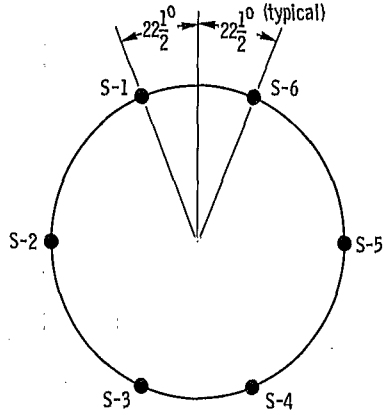

(b) Wall static pressure taps (station 8).

Figure 13. - General instrumentational locations.

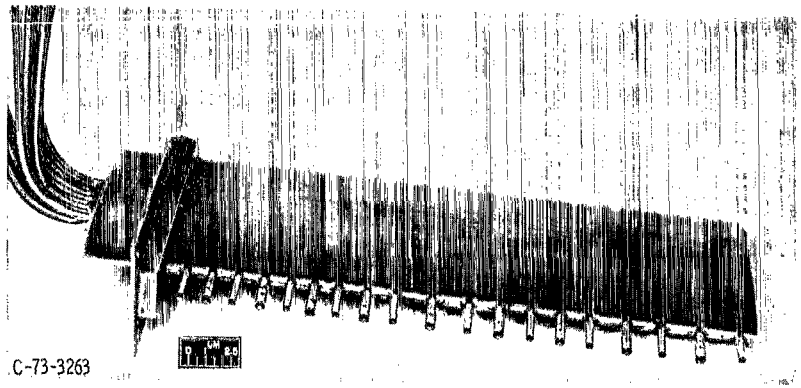

Figure 14. - Aerodynamic rake.

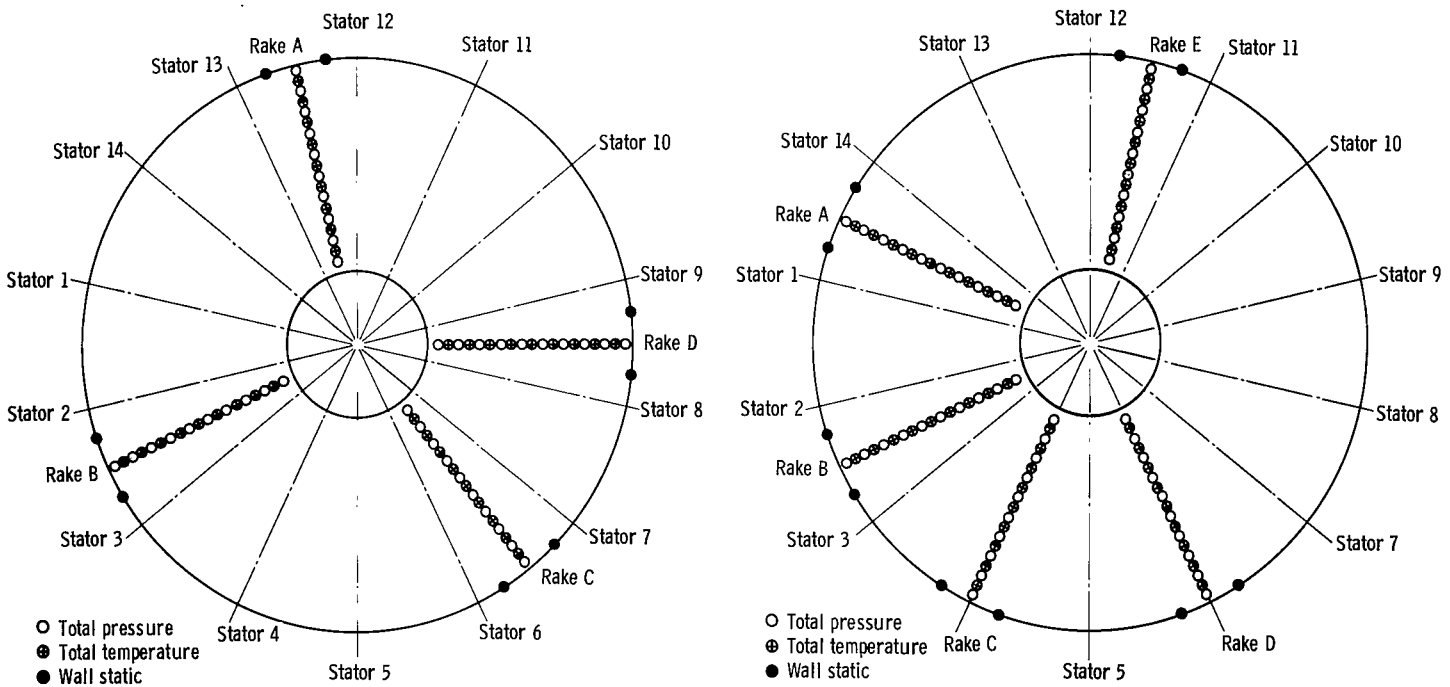

(a) Viewing downstream, station 3.

(b) Viewing downstream, station 4.

Figure 15. - Rake locations.

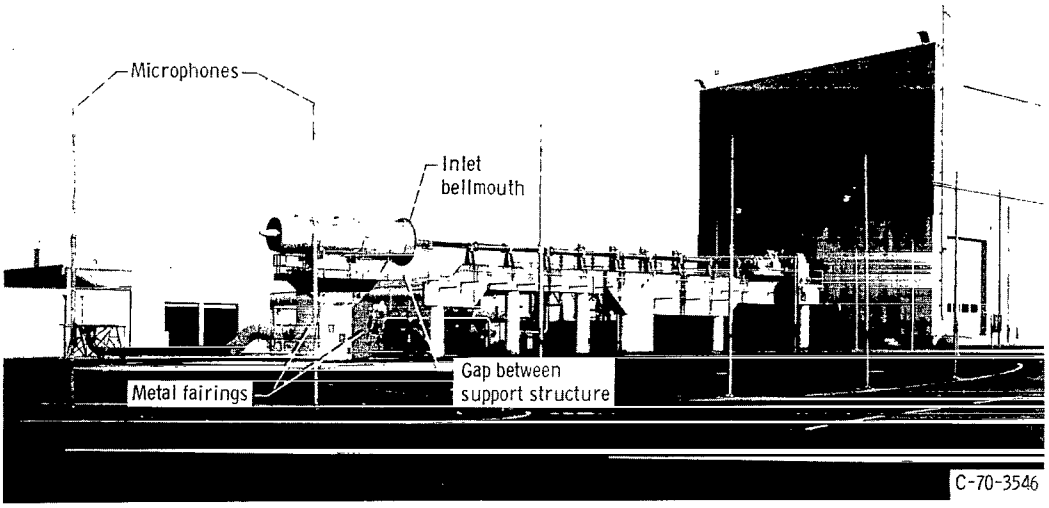

(a) Test site.

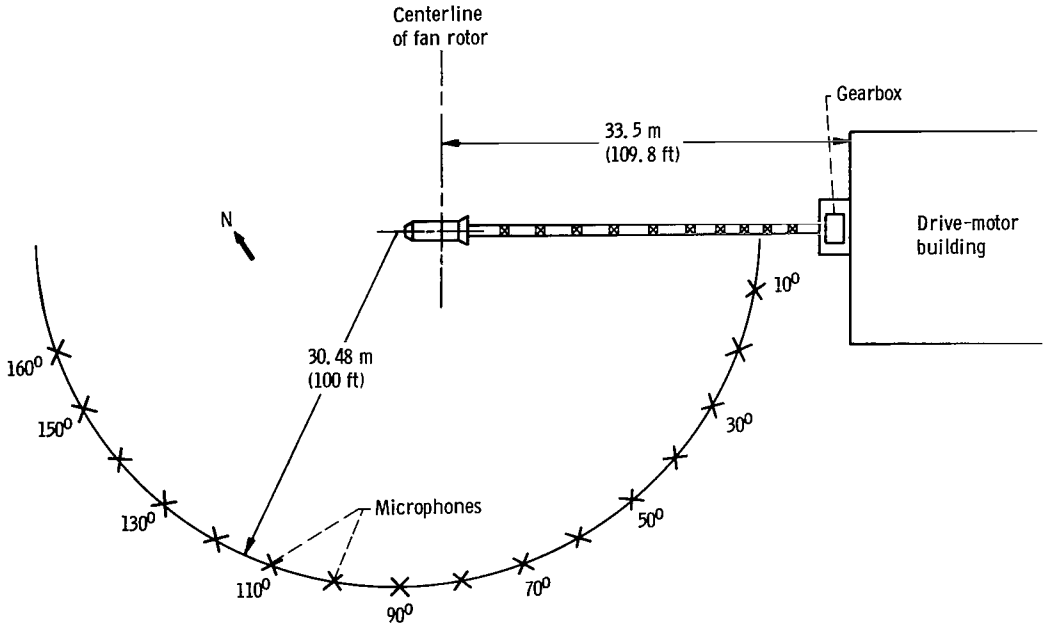

(b) Plan view of test site.

Figure 16. - Full-scale fan test facility.

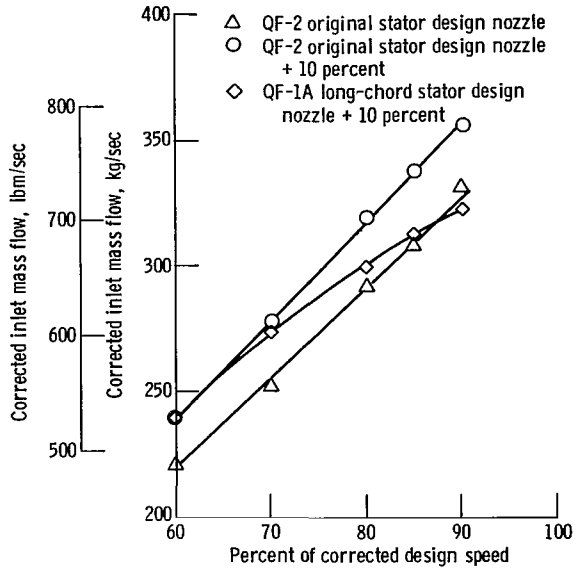

Figure 17. - Inlet mass flow.

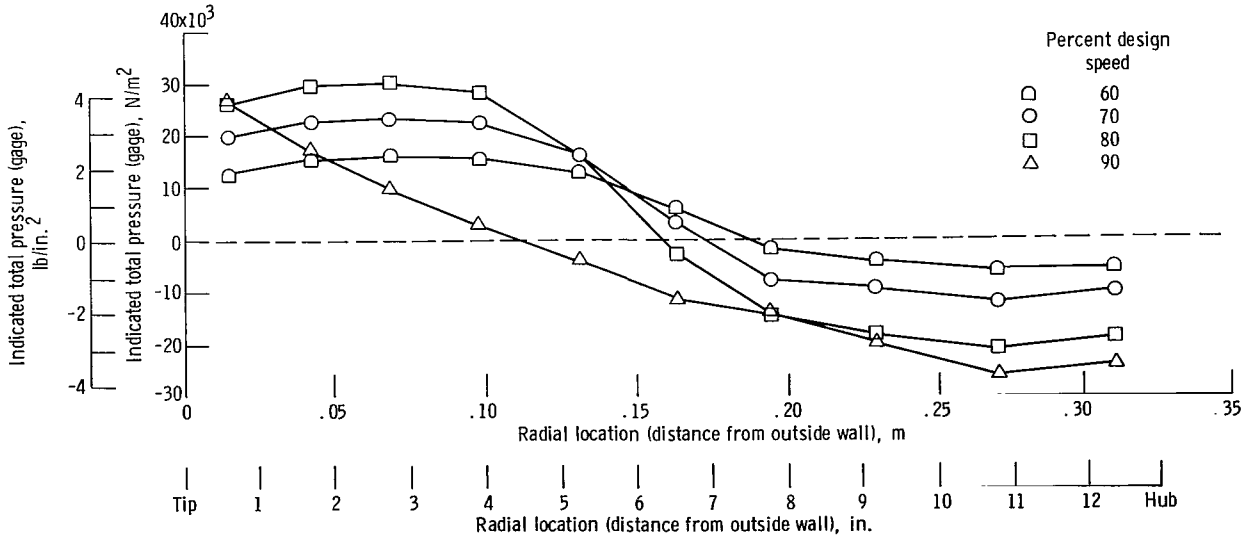

Figure 18. - Radial pressure (gage) measured with total pressure tubes near pylon at station 3 (rake C on fig. 15(a)).

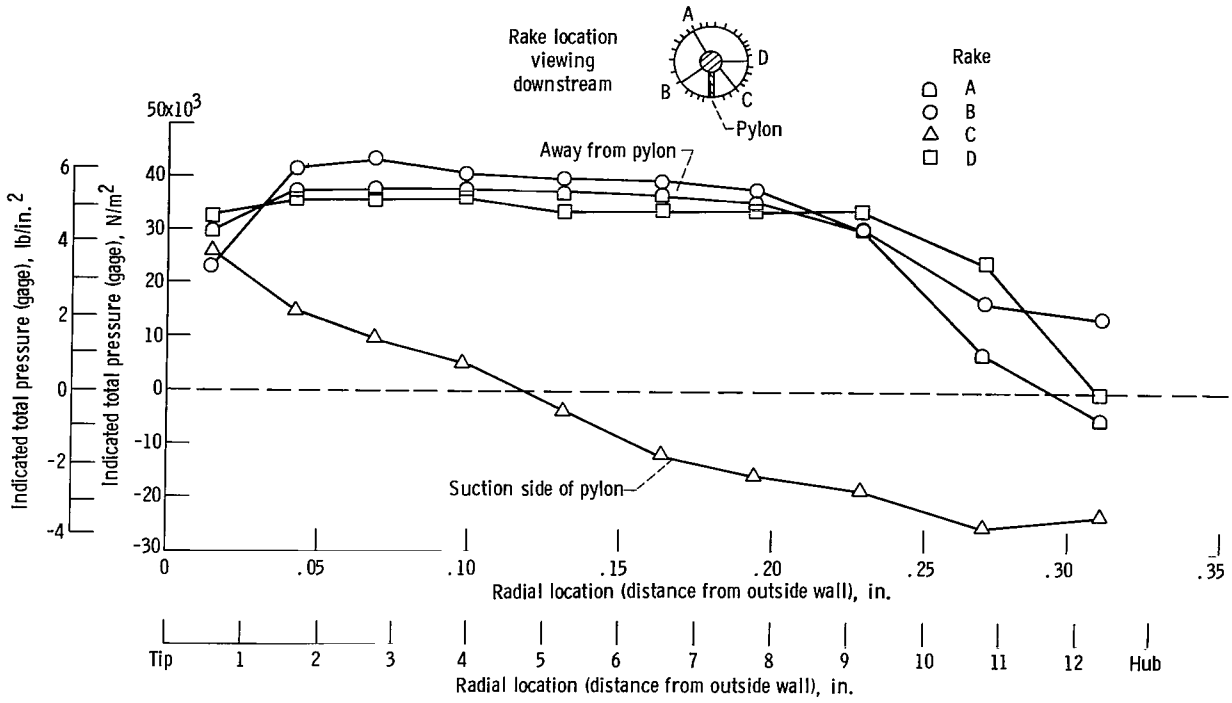

Figure 19. - Variation of pressure, measured with total pressure tubes, with radius from rakes at station 3 (see fig. 15(a)). Speed, 90 percent.

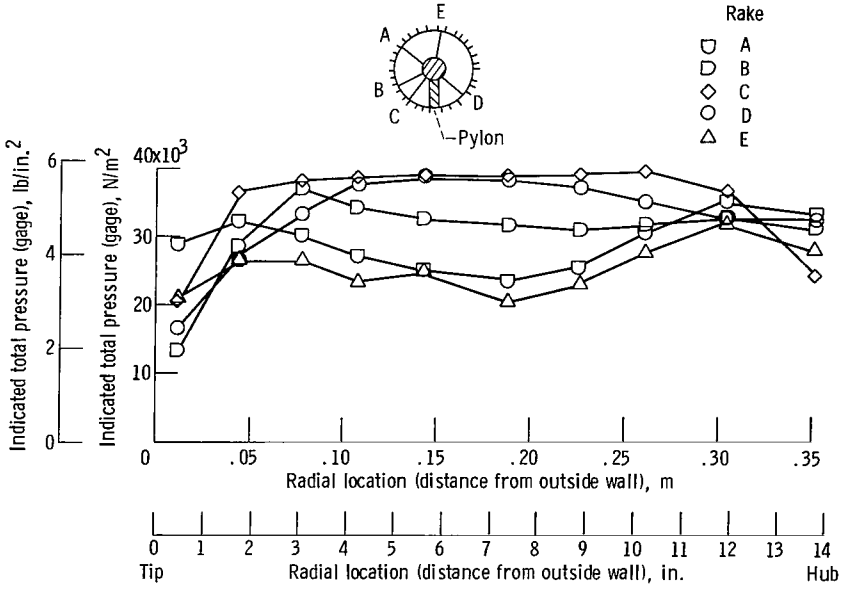

Figure 20. - Total pressure variation with radius from rakes at station 4 (see fig. 14(b)). Speed, 90 percent.

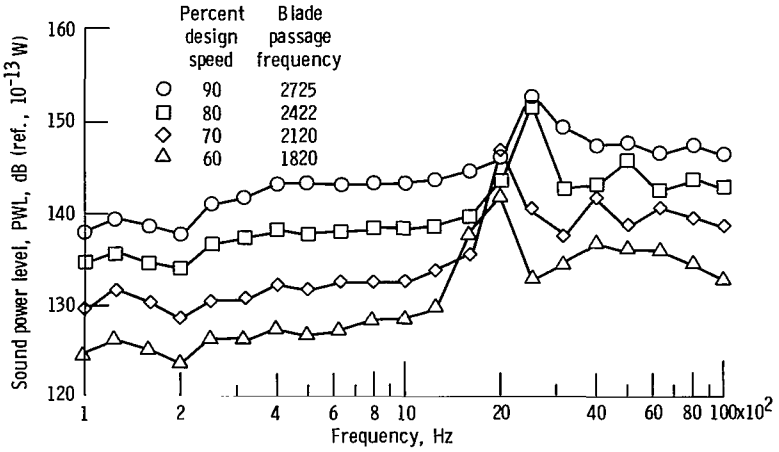

Figure 21. - One-third octave band acoustic spectra for longest stator configuration with cylindrical hardwall inlet.

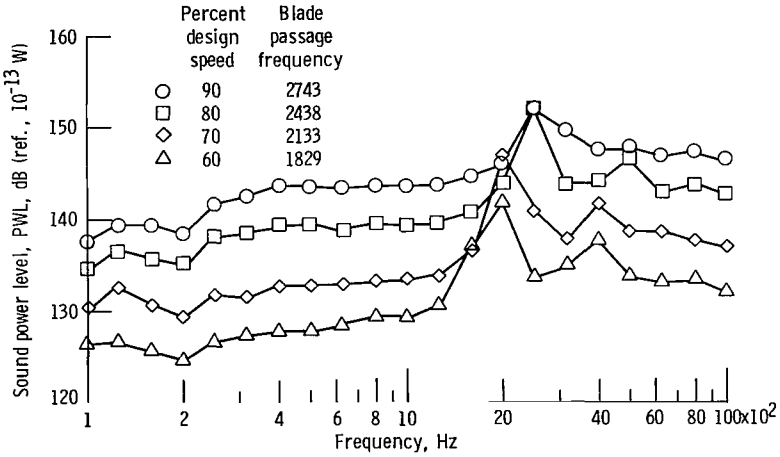

Figure 22. - One-third octave band acoustic power spectra for three-quarter stator configuration with cylindrical hard wall inlet.

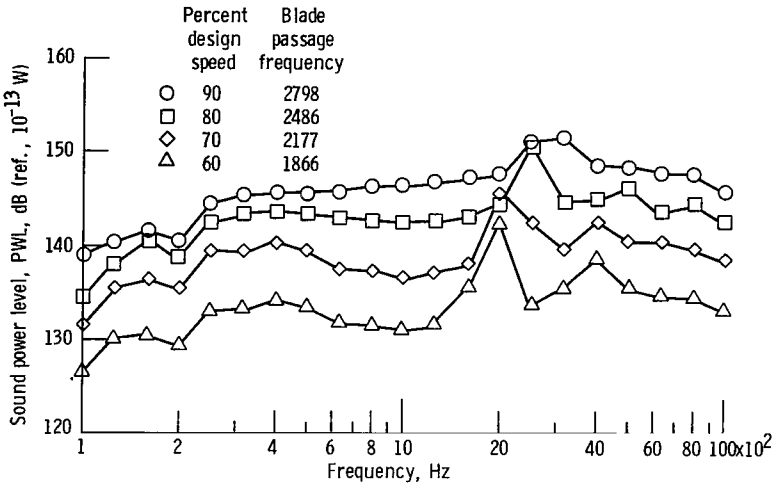

Figure 23. - One-third octave band acoustic power spectra for short stator configuration with cylindrical hard wall inlet.

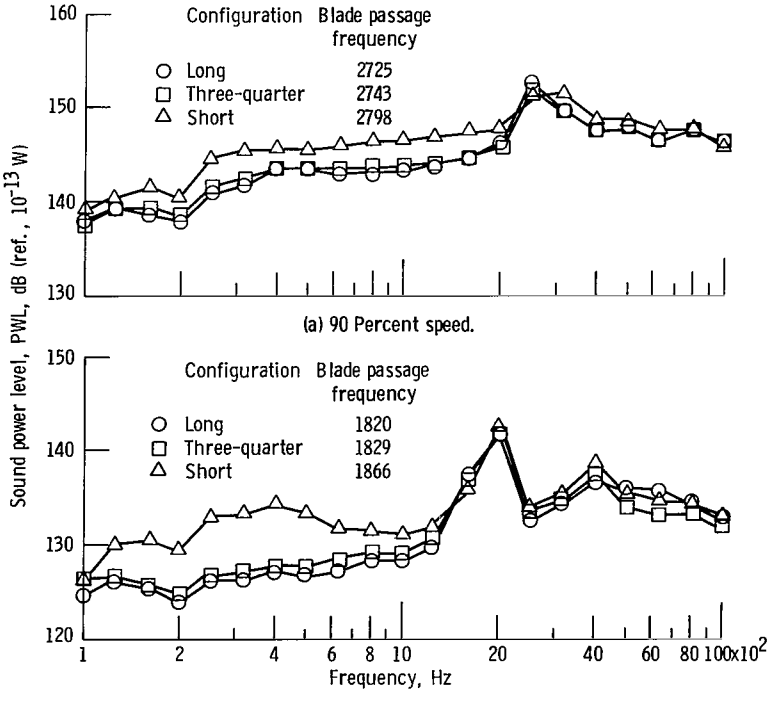

Figure 24. - Comparison of sound power level spectra for three lengths of long-chord stator.

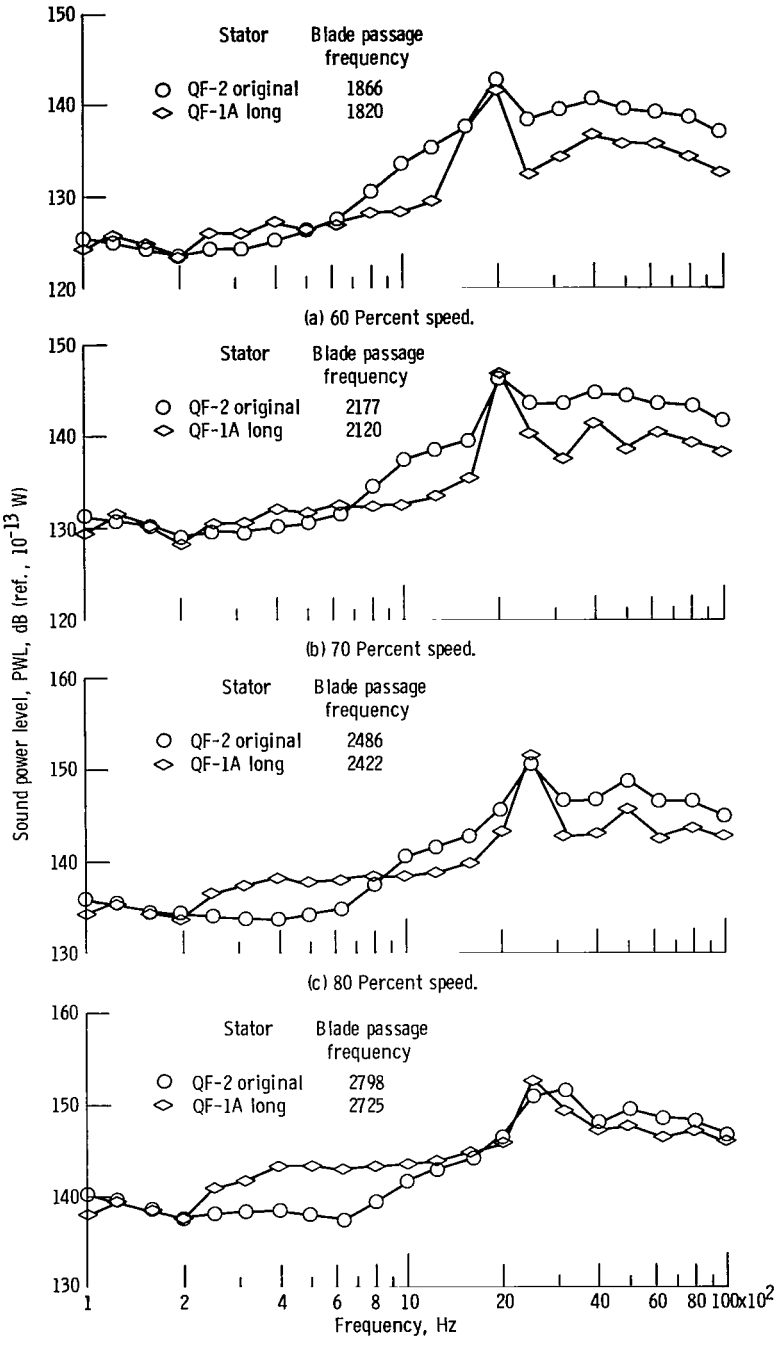

Figure 25. - Comparison of acoustic power spectra for longest configuration of long-chord stator and original QF-2 stator, cylindrical hardwall inlet.

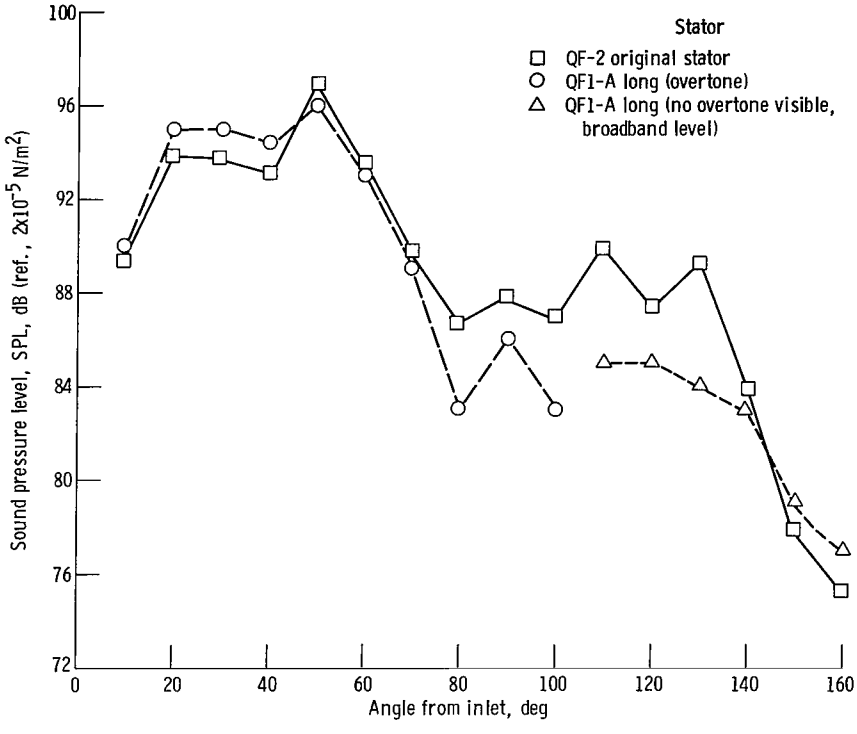

Figure 26. - Angular distribution of first blade passage overtone from narrowband spectra on 30.5-meter (100-ft) radius. Speed, 90 percent.

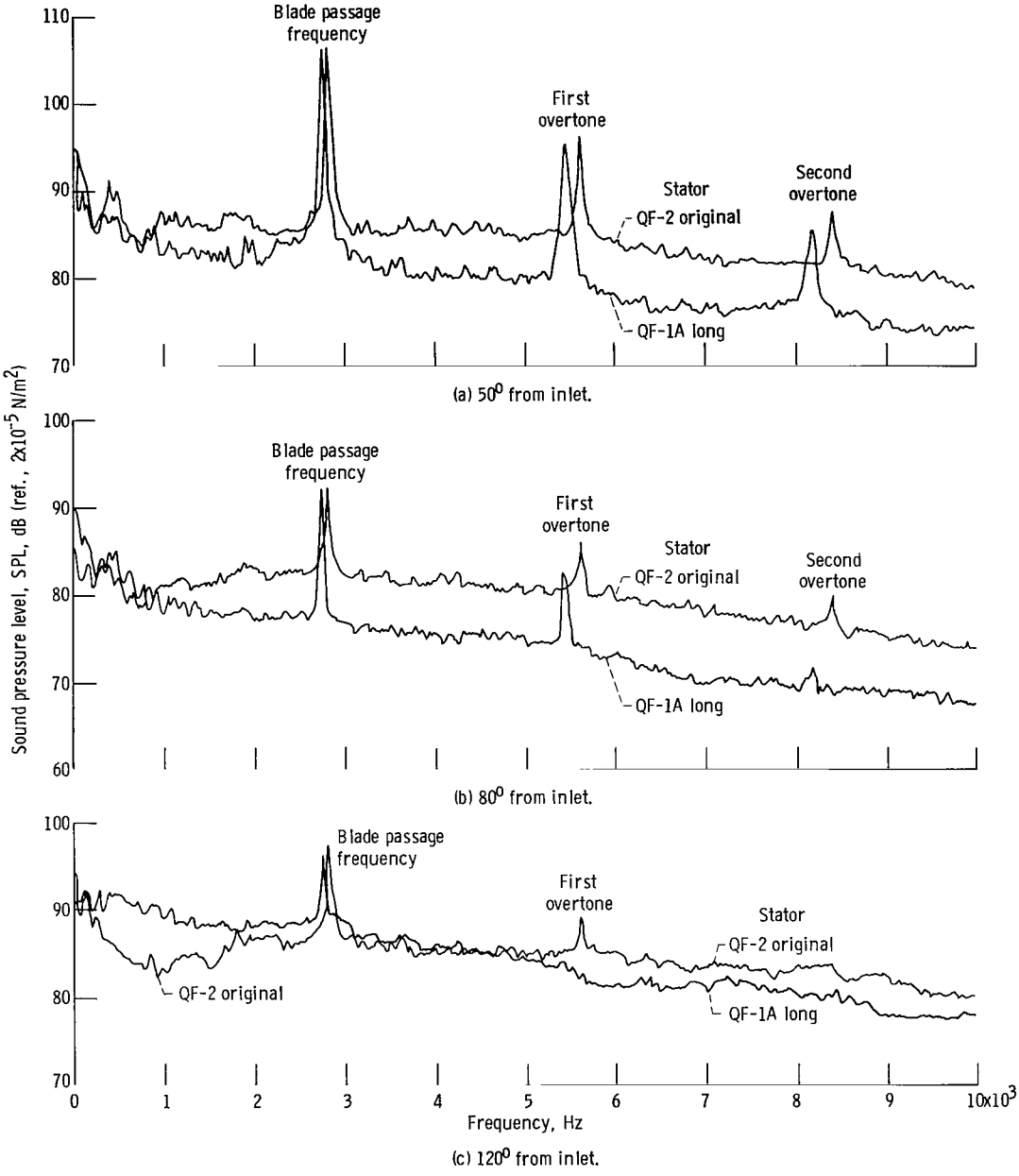

Figure 27. - Comparison of 10-hertz narrowband spectra at 90 percent speed.

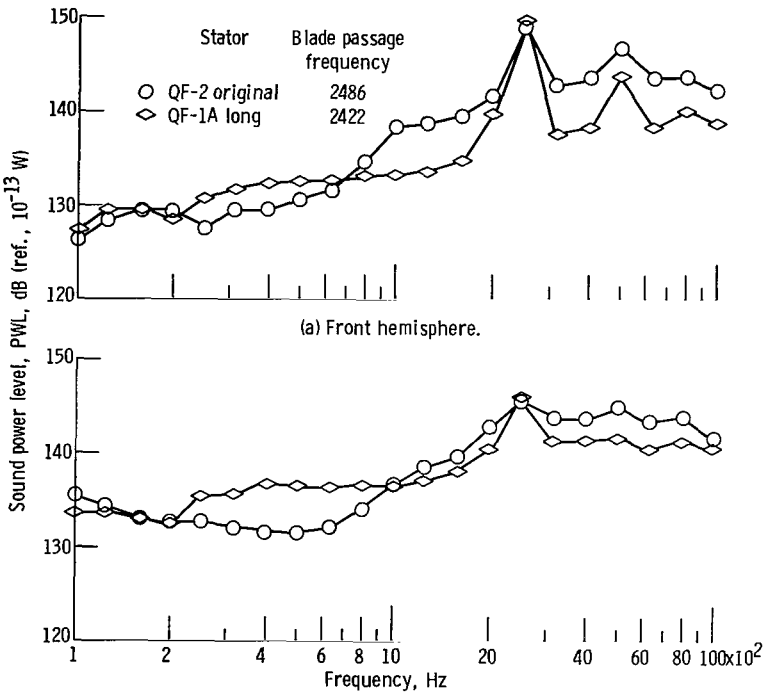

(a) Front hemisphere.

(b) Rear hemisphere.

Figure 28. - Sound power spectrum comparison at 80 percent speed.

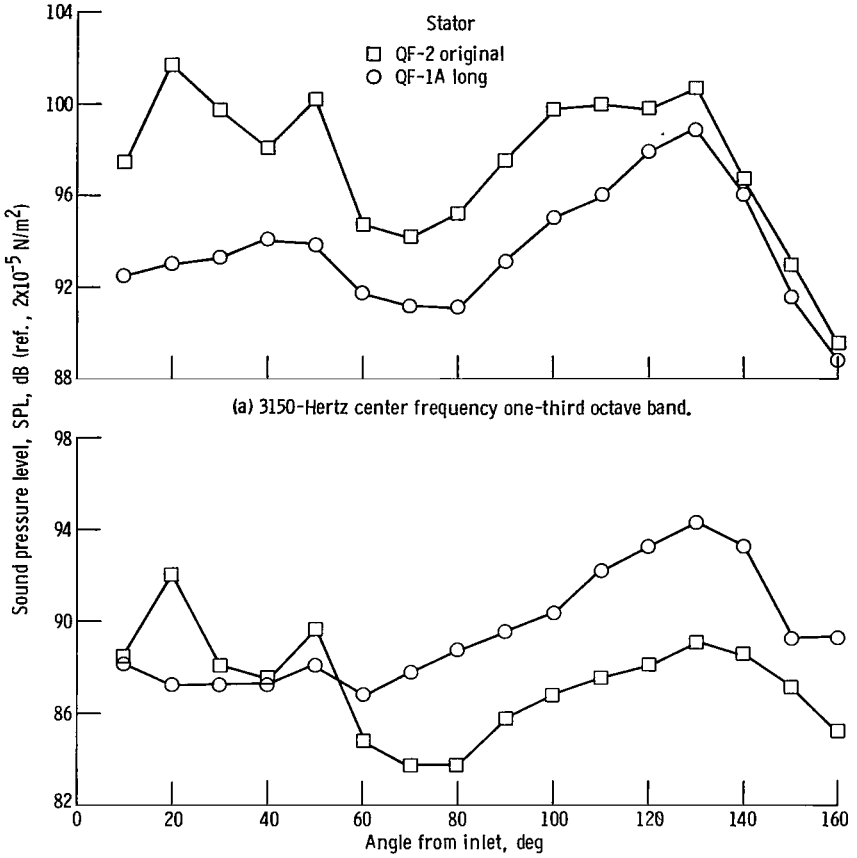

(a) 3150-Hertz center frequency one-third octave band.

(b) 630-Hertz center frequency one-third octave band.

Figure 29. - Sound pressure level comparisons with angle at 80 percent speed.

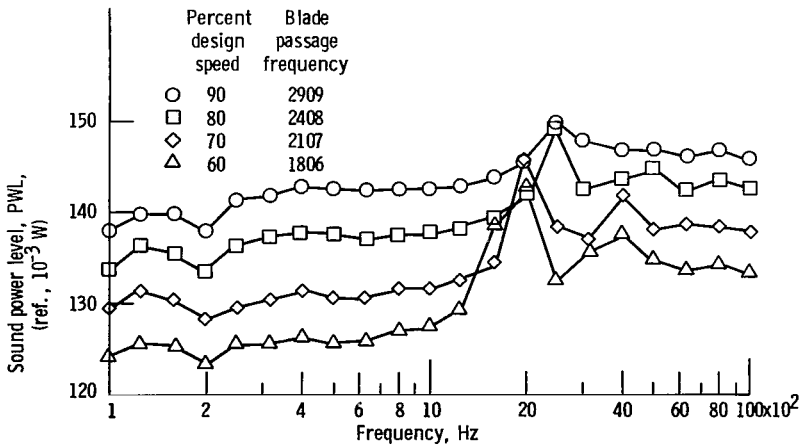

Figure 30. - Sound power variation with frequency for longest stator configuration with taped inlet and taped inlet splitter rings.

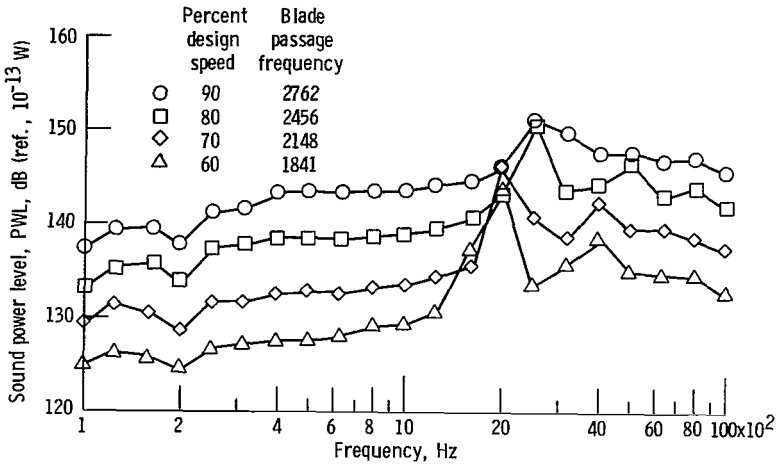

Figure 31. - Sound power variation with frequency for three-quarter stator configuration with taped inlet and taped inlet splitter rings.

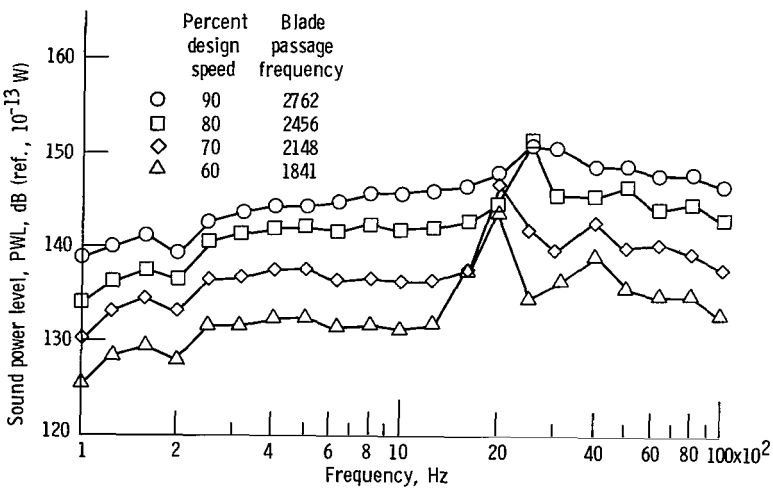

Figure 32. - Sound power variation with frequency for short configuration with taped inlet and taped inlet splitter rings.

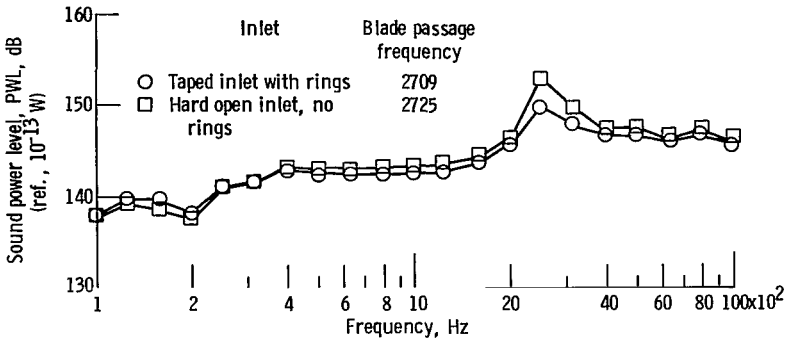

Figure 33. - Comparison of sound power at 90 percent speed for long stator hard open inlet with taped inlet and taped inlet rings.

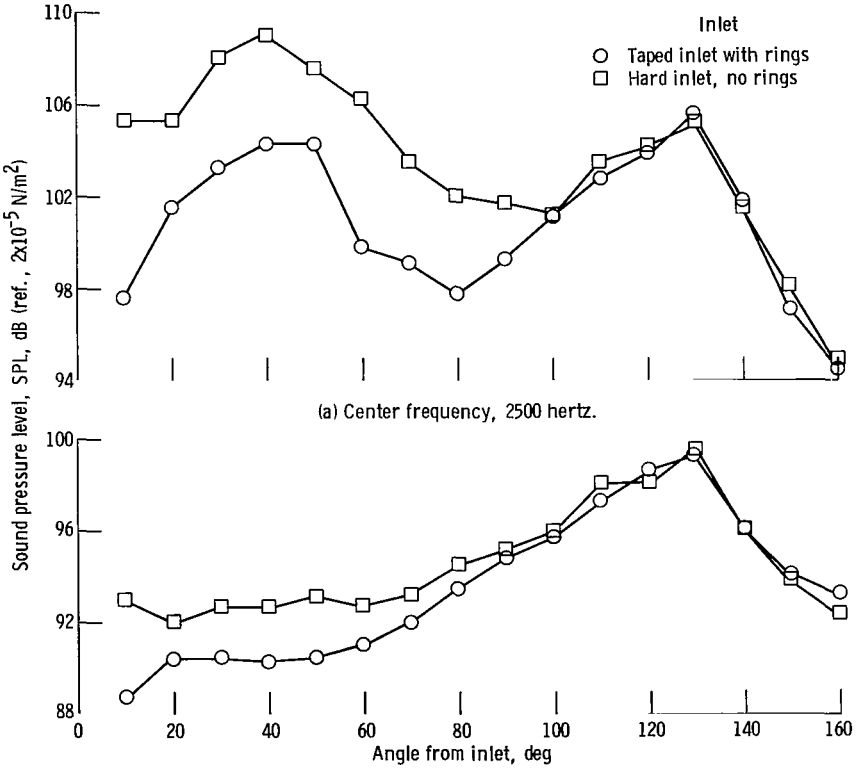

(a) Center frequency, 2500 hertz.

(b) Center frequency, 1000 hertz.

Figure 34. - One-third octave sound pressure level comparison with angle at 90 percent speed, long stator.

NATIONAL AERONAUTICS AND SPACE ADMINISTRATION
WASHINGTON, D.C. 20546

OFFICIAL BUSINESS
PENALTY FOR PRIVATE USE $300

SPECIAL FOURTH-CLASS RATE BOOK

POSTAGE AND FEES PAID
NATIONAL AERONAUTICS AND SPACE ADMINISTRATION
451

U.S.MAIL

990 001 C1 U A 751010 S00903DS
DEPT OF THE AIR FORCE
AF WEAPONS LABORATORY
ATTN: TECHNICAL LIBRARY (SUL)
KIRTLAND AFB NM 87117

POSTMASTER: If Undeliverable (Section 158 Postal Manual) Do Not Return

"The aeronautical and space activities of the United States shall be conducted so as to contribute . . . to the expansion of human knowledge of phenomena in the atmosphere and space. The Administration shall provide for the widest practicable and appropriate dissemination of information concerning its activities and the results thereof."

—NATIONAL AERONAUTICS AND SPACE ACT OF 1958

NASA SCIENTIFIC AND TECHNICAL PUBLICATIONS

TECHNICAL REPORTS: Scientific and technical information considered important, complete, and a lasting contribution to existing knowledge.

TECHNICAL NOTES: Information less broad in scope but nevertheless of importance as a contribution to existing knowledge.

TECHNICAL MEMORANDUMS: Information receiving limited distribution because of preliminary data, security classification, or other reasons. Also includes conference proceedings with either limited or unlimited distribution.

CONTRACTOR REPORTS: Scientific and technical information generated under a NASA contract or grant and considered an important contribution to existing knowledge.

TECHNICAL TRANSLATIONS: Information published in a foreign language considered to merit NASA distribution in English.

SPECIAL PUBLICATIONS: Information derived from or of value to NASA activities. Publications include final reports of major projects, monographs, data compilations, handbooks, sourcebooks, and special bibliographies.

TECHNOLOGY UTILIZATION PUBLICATIONS: Information on technology used by NASA that may be of particular interest in commercial and other non-aerospace applications. Publications include Tech Briefs, Technology Utilization Reports and Technology Surveys.

Details on the availability of these publications may be obtained from:

SCIENTIFIC AND TECHNICAL INFORMATION OFFICE

NATIONAL AERONAUTICS AND SPACE ADMINISTRATION

Washington, D.C. 20546